This document is supplied by QinetiQ for the MCA under contract No SEA00455

Research Project 572: Intact Stability Equivalent Criteria for Small Domestic Passenger Ships

A J Peters and D A Wing
QinetiQ/EMEA/TECS/CR0700506/v2.0
07 July 2008

Blank Page

Administration page

Customer Information	
Customer reference number	
Project title	MCA Research Project 572 – Intact Stability Equivalent Criteria for Small Domestic Passenger Ships
Customer Organisation	Maritime and Coastguard Agency
Customer contact	Mr D Foggie & Mr A Scott
Contract number	SEA 00455
Milestone number	3
Date due	23 July 2007

Principal author	
A J Peters	(023) 92 335217
Bldg 58 Rm 114A Haslar Marine Technology Park Haslar Road, Gosport Hants, PO12 2AG	AJPeters@QinetiQ.com
D A Wing	(023) 92 335221
Bldg 58 Rm 114A Haslar Marine Technology Park Haslar Road, Gosport Hants, PO12 2AG	DAWing@QinetiQ.com

Release Authority	
Name	J D Anderson
Post	Capability Leader, Surface Ships
Date of issue	

Record of changes		
Issue	Date	Detail of Changes
V0.1	June 2007	Draft Issue
V1.0	July 2007	Final Issue
V2.0	June 2008	Updated Issue

Blank Page

Abstract

Current intact stability standards required by EC directive 98/18 to be applied to seagoing passenger ships are soon to be required by SOLAS in respect of all conventional ships. In the case of small domestic passenger ships, various still water stability criteria are sometimes unattainable, such as the early peaking GZ curve criteria. This has led to the Maritime and Coastguard Agency (MCA) permitting some of these cases provided that other stability criteria are suitably upheld. The MCA wish to develop and validate the still water GZ curve criteria for these types of vessel, to ensure a level of safety equivalent to the International Maritime Organisation (IMO) Intact Stability Code (IS Code) is provided.

QinetiQ have considerable experience in this subject gained on behalf of the UK Ministry of Defence (MoD). Numerical simulations of extreme motions made using the state of the art dynamic seakeeping tool FREDYN are supported by zero-speed model tests in beam seas, which serve to add further validation to the numerical model.

Three different ships representative of modern forms were assessed for dynamic stability at a range of loading conditions. Utilising this data, the critical roll index of these ships in a number of loading conditions is then compared to features of the GZ curve to determine which static stability parameters have the greatest influence on the dynamic stability and what limits would provide an equivalent level of dynamic stability across modern designs. This allows the dynamic stability performance of the vessels to be related back to more easily measured static stability requirements which can be readily demonstrated by ship owners and operators, in submission to IMO regulations.

Blank Page

List of contents

1 Introduction

1.1 Background

1.1.1 The current intact stability standards that are required by EC Directive 98/18 to be applied to seagoing passenger ships on domestic voyages built post October 2002 (and to be phased in for earlier ships) replicate those soon to be required by SOLAS in respect of all conventional ships. The standards are contained in International Maritime Organisation (IMO) resolution A.749 [1]: the Code on Intact Stability (IS code).

1.1.2 There has been a significant focus on ship stability and capsizing in recent years. Empirical static stability criteria created from survival statistics of conventional hullforms are found to be inadequate for many small ferry designs, resulting in many otherwise stable designs being ruled 'unsafe' under the International Maritime Organisation (IMO) Intact Stability Code (IS Code) [1]. These failures are not due to the size of the vessels but as a consequence of their more extreme dimensional ratios. The beam/draught ratio (B/T), for example, is often outside the range of data which form the empirical basis for the criteria.

1.1.3 In the case of small domestic passenger ships, particularly those with open Ro-Ro decks and of a wide beam and shallow draft design, the various still water GZ curve criteria within A.749[1] are sometimes unattainable. The criterion most frequently failed by wide beam, shallow designs is that requiring the GZ curve to peak at an angle of heel beyond 25 degrees. As a result, MCA previously permitted early peaking GZ curves provided the energy criterion (area below the still water curve in m.rad) was suitably uplifted. Such 'equivalent' GZ curves had been allowed to have an angle of heel at the peak as low as 15 degrees in special cases.

1.1.4 At the SLF50 (Sub Committee on Stability and Load Lines and on Fishing Vessel Safety) meeting at IMO in May 2007, it was considered that the Offshore Supply Vessel rule, which compensates the reduced angle of maximum righting lever, down to 15 degrees, with an increase of dynamic stability (area under GZ) up to the maximum, was considered to be a viable alternative. There was also discussion on the equivalent level of safety that this ruling may provide. Currently there is no research to show that this ruling provides an equivalent level of stability performance.

1.1.5 It is widely accepted that a ship complying with the current IS Code rarely capsizes (reaches a critical roll angle) in non-breaking beam waves but could occasionally "capsize" when in following and quartering seas. Hence, to assess ship performance against capsize it is necessary to consider all ship headings [2]. To provide such an assessment of ship stability through model tests at a range of forward speeds, headings and realistic wave spectra would be prohibitively expensive and time consuming. Recent developments in modelling techniques and computing efficiency mean that numerical simulations now provide a fast and accurate alternative.

1.1.6 This task investigates and validates suitable still water GZ curve criteria which can ensure a level of stability performance comparable to the IS Stability code [1] when used with vessels with early peaking GZ curves. It is noted that such curves frequently exceed all the required criteria, by a significant margin, except angle of the GZ peak.

These findings could be applied to such ships whose proportions preclude the use of A.749[1] to provide a better understanding of their stability performance.

1.1.7 The alternative approach, which would require model testing of individual designs at their design stage and the making of individual submissions to the European Commission, is not believed to be an efficient solution.

1.2 Current & Previous Research at IMO on Intact Stability

1.2.1 The Stability, Loadline and Fishing vessel (SLF) subcommittee of IMO is currently reviewing and restructuring the Intact Stability Code (IMO Res. A749) with a view to making most of the standard GZ criteria mandatory for conventional ships. This IMO standard currently recognizes some ship types which may be assessed against specifically modified criteria sets. The offshore supply vessel criterion has been identified as an alternative for vessels with low peaking GZ curves.

1.2.2 Technology and knowledge are now beginning to reach a stage where different methods can be considered to provide a more realistic assessment of dynamic stability performance. The IMO is becoming receptive to the concept of accepting alternative proof of ship performance through such means. With this in mind it is necessary to ascertain the current level of dynamic stability and hence safety, ensured by the IS Code for conventional ships before applying these techniques to more novel hull forms.

1.3 Scope of this Investigation

1.3.1 The key objectives of this work were to:

- Conduct a literature review to identify similar research in this subject area.
- Compare performances of physical and mathematical models of a hull form of a candidate vessel in beam seas.
- Use a mathematical model to assess one conventional benchmark hull form and two wide beam variants.
- Investigate and develop GZ curve based criteria which can be applied to more extreme hull forms to ensure a level of capsize risk (taking 45 degrees as the critical roll angle for these vessels) and hence safety comparable with conventional hull forms under the IMO Intact Stability requirements (A.749).

1.3.2 A limited series of model tests has been performed in beam seas in order to investigate the dynamic stability performance of the conventional design. This allowed the comparison between the experiments and the extreme roll predictions made by the non linear time domain program FREDYN.

1.3.3 Following the model experiment comparison with the numerical predictions, the time domain program FREDYN was used to examine the three hullforms (one conventional and two high B/T hull forms). FREDYN was used to calculate the vessels' critical roll indices in a range of sea conditions, loading conditions, speeds and headings. The calculated indices (probabilities) of exceeding the critical roll angle were related back to static stability criteria, including those not currently considered in the IS Code. This established which parameters provided the best relationship to the dynamic stability performance in a seaway and also established suitable levels to ensure a prescribed level of dynamic stability performance for a range of vessel types at sea.

1.4 International Maritime Organisation Intact Stability Code

1.4.1 The latest Intact Stability code has the following stability requirements for conventional vessels. The IMO IS Code requires the following features of the GZ curve (restructured IS code [22]):

- The area under the GZ curve shall be not less than 0.055 m.rad up to 30° heel and not less than 0.09 m.rad up to the lesser of 40° or the angle of down-flooding,
- The area under the GZ curve between 30° and the lesser of 40° or the angle of down-flooding shall be not less than 0.03 m.rad,
- The maximum GZ shall be at an angle not less than 25°,
- GZ shall be at least 0.20 m at an angle of heel greater than or equal to 30°,
- Initial GM shall be not less than 0.15m.

1.4.2 The wind heeling criteria (Weather Criteria) are now mandatory for all vessels under the new IS code.

1.4.3 The ability of a ship to withstand the combined effects of beam wind and rolling should be demonstrated for each standard condition of loading. The Weather Criterion requires that area *b* should be greater than or equal to area *a* (see Figure 1-1). The angles and the main parameters are defined as follows:

ϕ_0 = angle of heel under action of steady wind

ϕ_1 = angle of roll to windward due to wave action

ϕ_2 = angle of downflooding ϕ_f or 50° or ϕ_c, whichever is less

ϕ_f = angle of heel at which openings in the hull, superstructures or deck-houses which can not be closed weathertight immerse

ϕ_c = angle of second intercept between wind heeling lever l_{w2} and GZ curves

l_{w1} = wind heeling lever

l_{w2} = 1.5 l_{w1}

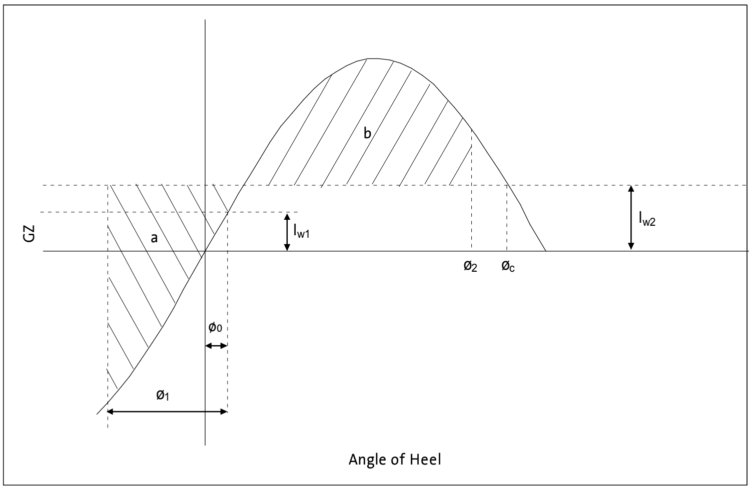

Figure 1-1 Weather Criterion Definition

The roll motion amplitude ϕ_1 in the Weather Criterion is calculated thus:

$$\phi_1 = 109kX_1X_2\sqrt{rs}$$

where:

k = empirical factor accounting for the effect of bilge keels on roll damping

X_1 = empirical factor accounting for the effect of B/T on roll damping

X_2 = empirical factor accounting for the effect of C_B on roll damping

r = effective wave slope coefficient, empirical factor accounting for wave exciting moment as a function of VCG and draught

s = correlation factor between wave period and wave steepness. Resonant rolling is considered as the failure mechanism hence the wave period is assumed to be ship's natural roll period

The wind heeling lever l_{w1} is constant for all angles of inclination and can be calculated as:

$$l_{w_1} = \frac{PAZ}{1000\Delta g}$$

where:

P = wind pressure of 504Pa (for wind speed 26 m/s), may be less for operation in restricted waters

A = projected lateral area of ship above waterline

Z = vertical distance from the centre of A to the centre of projected lateral underwater area

Δ = ship displacement in tonnes

g = acceleration due to gravity, 9.81 m/s²

Alternative means of determining the wind heeling lever may be accepted by the IMO administration.

1.4.4 Offshore supply vessels are one example where special dispensation is required since many of these vessels have early peaked GZ curves. That is, the maximum GZ occurs at a heel angle less than 25°. In such cases section 2.4.5.2 of the Restructured IS Code [22] applies:

- The area under the GZ curve of righting levers (GZ curve) should not be less than 0.070 metre-radians up to an angle of 15 degrees when the maximum righting lever (GZ) occurs at 15 degrees and 0.055 metre-radians up to an angle of 30 degrees when the maximum righting lever (GZ) occurs at 30 degrees or above. Where the maximum righting lever (GZ) occurs at angles of between 15 degrees and 30 degrees, the corresponding area under the GZ curve should be :

$$0.005 + 0.001(30° - \emptyset_{max})\ \text{metre-radians}$$

- The area under the righting lever curve (GZ curve) between the angles of heel of 30 degrees and 40 degrees, or between 30 degrees and $\emptyset_f$ if this angle is less than 40 degrees, should not be less than 0.03 metre-radians.

- The righting lever (GZ) should be at least 0.2m at an angle of heel equal to or greater than 30 degrees.

- The maximum righting lever (GZ) should occur at an angle of heel equal to or greater than 30 degrees.

- The initial transverse metacentric height (GM) should not be less than 0.15m.

Blank Page

2 Literature Review

2.1 Review

2.1.1 A literature review was undertaken during the early stages of the project and subsequently provided to the MCA. It is also repeated in the following sections (Sections 2.2-2.7). A section on naval stability standards has also been included in this report (Section 2.8).

2.2 Development of the Weather Criterion

2.2.1 Francescutto and Serra [3] provide an account of the development and applicability of the IMO Weather Criterion to modern large passenger vessels. The source of the current formulation is reviewed, and the major shortcomings in the method are identified. The process is considered to be broadly valid however limitations are identified in extending the method to modern designs, where the limits of the original data are exceeded. The main reported failing of the Weather Criterion is in the estimation of roll motion amplitude, discussed below.

2.2.2 The factors k and X_2 are related to the effect of bilge keels and block coefficient on roll damping, and are suited to modern forms. X_1 and r have major influences on stability, and in many cases the formulations used do not cover the range of dimensions typical of modern ships. The factor X_1 accounts for the effect of B/T on roll damping; the original data cover a range of B/T from 2.5 to 3.5. Many modern passenger vessels fall outside this range; Eliopoulou and Papanikolaou [4] report B/T ratios of small ferries built post 1990 between 3.6 and 4.9. Ships with B/T greater than 3.5 are assumed to follow the last available value (Figure 2-1) – an assumption which introduces considerable error when considering high B/T ships.

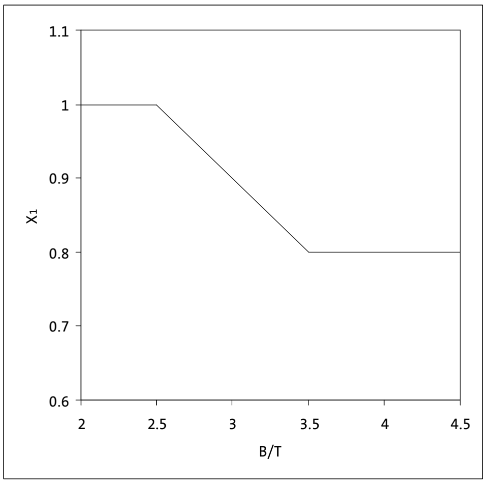

Figure 2-1 Effect of B/T on Weather Criteria

2.2.3 The effective wave slope coefficient, r, which accounts for wave exciting moment as a function of VCG and draught, is also found to be inaccurately represented in the weather criterion resulting in its over prediction for small ships. It is concluded that the combined effect of these inadequacies over predicts the influence of environmental action for modern, high B/T forms, leading to many failing the current criteria. A further failing is in the definition of roll period, which affects factor *s*, accounting for wave steepness at roll resonance. The formula has provision for roll periods up to 20 s, while many modern passenger vessels may have natural roll periods up to 30 s.

2.2.4 This work received further study from Francescutto and Serra [5] covering model tests to determine suitable ranges of roll damping and effective wave slope coefficients for ships having large B/T, OG/T and roll period. These confirmed the inaccuracy of roll period and effective wave slope coefficient estimates made using the IMO Weather Criterion. A modification to the effective wave slope coefficient was suggested to better cover such ships.

2.2.5 Cramer and Tellkamp [6] aim to provide a basis for the evaluation of a ship's intact stability based on performance criteria and direct assessments and with it suggest revisions to the approach of the IMO Intact Stability Code, from being a prescriptive code to a goal-based approach. It is reported that the current dynamic intact stability criteria do not reward improvements in the stability of a design, and in some cases can punish improvements even if model tests or simulations display greater safety (e.g. the addition of roll damping devices such as flume tanks is punished by excessive free surface moment corrections should the control mechanism fail without taking into account benefits in normal operation). It is suggested that this is a result of the origin of the criteria in design data from years past, and the inapplicability of this data to modern vessels. The current dynamic stability requirements are simply based on static stability in calm water with no allowance for real dynamic behaviour and so are inherently flawed.

2.2.6 It is recommended by Cramer and Tellkamp [6] that some means of direct assessment of dynamic stability is allowed, and that the criteria used to assess safety are performance based rather than empirical. The numerical tools and model test techniques currently available are found to predict, with some confidence, dynamic stability properties when used appropriately. Some uncertainty remains over the level of safety represented by existing rules, leading to difficulties in defining a degree of safety for the updated approach.

2.2.7 An 'equivalent safety' method of ship design is presented, in which the stability of a design is not considered *per se*; instead a qualitative comparison of different ships is used. The results of numerical testing are reported, using the 'safe' or 'unsafe' criteria developed by Blume [7], as polar plots of the maximum significant wave height in which the ship is classed as 'safe' for a range of ship speeds and headings. These are used to determine problem areas of operation, however the difficulty of directly comparing different designs in different loading conditions and wave spectra is recognised. It is noted that a change in philosophy is required to assess future designs, but that in doing so a level of safety to be attained must be determined.

2.3 Modifications to the Weather Criterion

2.3.1 As an interim measure it has been recommended in [8] that the Weather Criterion be updated to cover a wider range of vessel dimensions by modification of the factors *r* and *s*, and through an alternative assessment of the roll period by model testing or full scale trials. The suggested alteration is to be incorporated as an interim measure only until it can be more fully assessed. Additional data from experimental studies are provided in [9], [10] supporting this recommendation for updates to the IS code.

Japan [11] provides details of the development of the Weather Criterion, which has its roots in the Japanese stability standards for passenger ships.

2.3.2 In [12], Francescutto provides an account of the development of current stability rules, and suggests a new direction utilising state of the art numerical and scientific tools. As part of this Francescutto further recommends amending the factors *r* and *s* as an interim measure to improve the level of validity to modern ships, also suggesting that these values and others used in the Weather Criterion may be obtained from model testing or numerical simulations where appropriate.

2.3.3 Turan and Tuzcu [13] report the failings of modern stability rules to cover the range of dimension ratios appropriate to current vessels. The paper looks at some of the issues regarding recent developments in performance-based approaches to the stability of cruise vessels. The importance of ensuring that future frameworks are “developed in such a way that assessing alternative designs and arrangements so as to ease the approval of new concepts and technologies which provide a level of safety at least equivalent to that provided by the prescriptive regulations” is stressed.

2.3.4 In [13] the Weather Criterion is applied, in the original formulation and in its modified form to a test case cruise vessel having B/T = 4.0 which fails the original criteria in some loading conditions. It is found that the modified criterion results in the limiting GM curve being less severe, meaning the loading conditions which had failed the criteria are able to pass. The primary region of non-compliance is found at the lighter draught range. It is accepted that the modifications improve compliance for such forms, but the inherent limitations of the theory mean it cannot truly reflect the level of safety of these ships. It is recommended that the modified Weather Criterion is studied further to eliminate the artificial non-compliance of some passenger ships.

2.4 Validation of the Weather Criterion through Experimentation

2.4.1 Yoon *et al* [14] report the results of model testing to assess the validity of the Weather Criterion in its older, empirical form and the proposed alternative method incorporating model tests. The study looked at the wind heeling lever by measuring the location of the centre of underwater lateral resistance through drifting tests at various angles of heel. In addition, tests in beam seas were carried out to estimate roll-back angles. The model tested was scaled to fit IMO guidelines of minimum length 2.5m, and to avoid shallow water effects on wavelength. The dimensions fall outside the range of ships for which the older method of determining Weather Criterion is considered valid, having B/T = 3.94 and OG/T = 0.84 whereas maximum recommended values are 3.5 and 0.5 respectively. These ratios are within the dimensions suggested for the alternative improved method.

2.4.2 In [14] a clear case is made for the revision of the empirical determination of the hydrodynamic lever, showing that this quantity varies with heel angle. In the case of large heel angles the vertical hydrodynamic force acting on the hull is asymmetric resulting in the virtual centre of drift force being above the waterline. This is in direct contradiction to the Weather Criterion estimate which assumes the drift force acts at half draught below the waterline and remains constant throughout the range of heel angles. This phenomenon is especially important for ships with high B/T as the influence of bottom pressure increases compared to that of the side pressure.

2.4.3 Taguchi *et al* [15] and Ishida *et al* [16] report a similar series of model experiments to measure wind heeling lever and roll angle. The vessel used is a RoPax ferry with B/T = 3.8. The primary results confirm that the wind heeling lever is a function of the roll angle and that the hydrodynamic force due to hull drift differs considerably from the empirical method for hulls with high B/T ratios. The Weather Criterion is considered in light of various combinations of these experimental data and empirical relationships, and a range of critical KG values derived accordingly. It is found that up to 0.4 m (4.4%) variation exists in this KG range, the primary cause of which being the variation in vertical centre of lateral resistance found from the drift tests. An iterative approach to determining KG requirements may be more appropriate due to the effect of KG on roll period and other factors related to roll motion.

2.4.4 It should be noted that neither Yoon *et al* nor Ishida *et al* directly consider the resistance to capsize of such forms through model testing or numerical simulations, but do demonstrate the inadequacies of the Weather Criterion.

2.5 Validation of the Weather Criterion through Numerical Simulations

2.5.1 Vassalos *et al* [17] report the results of numerical simulations of ship behaviour in wind and waves, based on a six degree of freedom time domain model. The primary focus of this study is in determining the relevance of the weather condition defined in the IMO Weather Criterion, and how this corresponds to the expected roll angles resulting from such conditions. The capsize risk of modern passenger vessels is not considered within this study. It is found that the underlying assumptions used in the weather criterion are broadly valid, but the likelihood of occurrence of the relevant conditions in combination is low, and it is recommended that the criterion is revisited using modern techniques and knowledge of ship stability.

2.5.2 Matusiak and Hamberg in [18] compare the maximum roll angle of a passenger ship as predicted by the IMO Weather Criterion against the six degree of freedom non-linear seakeeping code LAIDYN. The numerical model is used to obtain the maximum roll of the ship by simulation of the conditions which form the Weather Criterion. The simulation is performed in beam waves with gusty wind acting as specified in the Weather Criterion, and additionally in calm water with an initial roll angle as determined by the simulation in waves. It is argued that in the resonance condition the wave loading and roll damping compensate themselves, and it follows that only the initial conditions have an effect on the maximum angle and the continued wave excitation can be neglected. This is confirmed by numerical simulations as the two methods give similar results for the maximum roll angle.

2.5.3 It is suggested that the modelling of unsteady hydrodynamic radiation forces resulting from sway acceleration can significantly affect the maximum roll angle response of the vessel, and consequently numerical tools are recommended as a means of assessing the safety of a design.

2.6 Direct Assessment of Capsize Probability through Numerical Simulation

2.6.1 Perhaps the closest previous study to this current investigation, is that of Cramer *et al* [19], and the related works of Krueger and Kluwe [20],[21]. In combination they present an account of the development and application of a suggested structure for dynamic stability criteria using a probabilistic approach.

2.6.2 Both note that intact stability and hence resistance to capsize is not solely a function of GM, and must account for dynamic situations such as broaching; this cannot be avoided by modifying GM. It is recommended that future approaches to dynamic stability regulations should cover:

- criteria to avoid large rolling angles (minimum stability requirement),
- criteria to avoid large accelerations (maximum stability limit),
- criteria to guarantee sufficient roll damping in dead ship condition (minimum damping requirement),
- criteria to avoid broaching (minimum course keeping requirement).

2.6.3 Large accelerations are defined as any acceleration which causes cargo loss, damage to the ship or systems or discomfort and injury to the crew and passengers. It is noted that such accelerations are not necessarily accompanied by large amplitude roll motions. Clearly, dynamic numerical or model simulations are well suited to the necessary analysis of accelerations.

2.6.4 It is noted that improving the stability of small ferries in head or following seas through increasing GM can have negative effects on the stability in beam seas. In beam seas, small ferries with relatively high GM can suffer capsize as the ship's natural roll frequency matches the encounter frequency, and wavelength approximates ship beam. This is not as important for large vessels as the GM values which fulfil these conditions are very large, or the critical waves are not sufficiently high. Thus it is difficult to reach a generalised conclusion on GM values which provide adequate stability. Due to this relationship the risk of capsize in beam seas and bow quartering/following seas should be treated separately, with GM criteria formulated accordingly.

2.6.5 Both texts detail the results of simulations to determine a capsizing index, in a similar manner to Cramer and Tellkamp [6], for various modern ship types using the six degree of freedom program 'ROLLS'. All ships were studied at the design draught, and at the limiting GM value according to the IMO IS Code. Further conditions with increased GM are also tested.

2.6.6 The calculated capsize index is weighted for the likelihood of occurrence of sea state, vessel course and speed causing capsize, and the results then compared to various static stability parameters. The method makes no account of the influence of the operator in avoiding dangerous conditions, and similarly assumes all ships operate in the same wave conditions. Based on the data the following conclusions were reached:

- the current code on intact stability does not represent a unique safety level because low GM ships can exhibit high safety and *vice versa,*
- the ships whose failures result from pure loss of stability on a wave crest show a large improvement in safety if GM is slightly increased,
- the ships characterised by parametric roll and/or excessive heeling moments need larger increases in GM to achieve the same safety level,
- some ships cannot go beyond a certain safety level even if GM is significantly increased as stability is a function of righting lever alteration, which is a function of the hull form only,
- most of the ship types which represent more traditional designs such as bulkers and tankers seem to be very safe whereas modern ferries and

ROROs have significant problems due to large righting lever alterations between trough and crest conditions.

2.6.7 When considering the level of safety provided by ships operating at the limit of the current IMO IS Code there is considerable variation in the results. When capsize index is plotted against still water GM there is large scatter in the data. This supports earlier findings that the rules based on GM do not guarantee a uniform level of safety across a range of ship types, and that GM in itself is not a suitable variable to define rough weather stability.

2.6.8 It is shown that the occurrence of large roll amplitudes is closely linked to crest/trough alterations in area under the GZ curve, and it is suggested that modified criteria may be based on these alterations. In particular, it is found that the ratio of difference in area under the GZ curve between crest and trough condition to the area under the GZ curve in still water is important. It is then noted that alteration of the GZ curve in the crest/trough condition is mainly dependent on the hull form and not on the initial GM, and so the aim of the criteria should be to ensure the area under the still water GZ curve is sufficient to compensate for the crest/trough alterations of the specific hull form. This can be achieved by increasing GM, or alternatively, at the design stage it is possible to alter the hull form to reduce the variation between crest and trough condition.

2.6.9 The results presented do provide some qualitative guidance on how to improve the level of safety against capsize. It is noted that the safety of ships is always improved if the degree of alteration in GZ curve between the wave crest and trough situation is minimised. Contrary to traditional views of stability it is found that increasing GM does not, in itself, guarantee improved stability for many hull forms.

2.6.10 Krueger and Kluwe [20] present the results of systematic simulations to assess the effect of roll damping on a single hull form. It is found that the addition of bilge keels to a ship decreases capsize probability significantly, but the provision of larger bilge keels than usually specified has very little further benefit. Therefore, it is more appropriate to define a minimum level of roll damping which must be attained than to allow a GM reduction to vessels having a greater degree of roll damping.

2.6.11 A simplified probabilistic intact stability criterion is developed, based on the simulated data above. The criterion uses the difference ratio mentioned earlier applied to the area under the GZ curve to 40° and to the maximum righting lever:

$$p_{\text{capsize}} = 1 - \sqrt{\left[\frac{A_{40} / A_{40\,\text{DIFF}}}{k_1}\right]\left[\frac{h_{\max} / h_{\max\,\text{DIFF}}}{k_2}\right]}$$

where:

A_{40}	= area under the GZ curve to 40°
A_{40DIFF}	= difference in area under GZ curve between crest and trough
h_{max}	= maximum GZ
$h_{maxDIFF}$	= difference in maximum GZ between crest and trough
$k_{1,2}$	= tuning factors to fit experimental data.

It is suggested that $k_1 = k_2 = 0.7$ is a reasonable fit to the simulated data.

2.6.12 Capsize probabilities are calculated for the test ships using this method, and found to compare well with the capsize probabilities from simulations – considerably better than the current GM based criteria. It is suggested that the $k_{1,2}$ values chosen are not suited to all ships, and should be adjusted for particular ship types and operating sea spectra. The variable A_{40DIFF} is found to vary considerably according to how the reference wave is defined, and it is suggested that a range of reference waves are used [21].

2.6.13 The simplified criterion is applied to four test ships (RORO, container, bulker and gas tanker) for a range of GM. It is found that the RORO vessel has the lowest safety level of all those considered, and that only the IMO Weather Criterion provides some degree of safety for such ships. In all cases the limiting GM for damage stability is found to indirectly increase the intact stability level in practice. It is suggested that the probabilistic criterion can be improved through a more representative definition of the speed profiles concerned and subsequent recalculation of the parameters $k_{1,2}$.

2.7 Stability of Unconventional Forms

2.7.1 A number of marine vehicles which do not display conventional stability characteristics are covered by exemptions or alterations within the IMO IS Code. Offshore supply vessels are one example of such special dispensation as many of these vessels have early peaked GZ curves. That is, the maximum GZ occurs at heel angle less than 30°. In such cases section 2.4.5.2 of the Restructured IS Code [22] applies (see section 1.4.4 above).

2.8 Naval Stability Standards

2.8.1 The range of approaches to determining and assessing intact stability of naval vessels is summarised by Hughes [23]. As is found in commercial applications of stability criteria the shape of modern warships is becoming increasingly dissimilar to that of the vessels on which the criteria are based. For warships the most significant study of naval stability results from a study by Sarchin and Goldberg based on 'intact' capsizes of three US destroyers in a Pacific typhoon in 1944 [24]. The reasons for questioning the validity of these standards to more modern forms are also similar:

- the applicability of quasi-static methods to dynamic behaviour in extreme conditions is questionable,
- modern naval hull forms are increasingly dissimilar to those on which stability criteria are based, and are susceptible to capsize risk in different conditions to those which threaten more traditional forms,
- the level of safety assured by current standards is essentially little known.

2.8.2 With advances in modern computational capability and hydrodynamic techniques these standards are being reviewed with the aim of developing criteria directly based on capsize risk. In particular there is an aim to answer the following questions:

1. What probability of capsize is currently accepted through application of the Sarchin and Goldberg [24] based criteria?
2. Does the application of these standards to modern hull forms result in a significantly different probability of capsize?
3. What is the range of validity of these standards for different modern hull forms?

4. How should the stability of modern vessels be assessed if the current criteria and quasi-static approach is no longer valid?

Considering warship design the problem of through-life stability management becomes more prevalent. It is generally easy to achieve compliance with stability standards at the start of a warship's life, however this compliance becomes more difficult as displacement and KG gradually increase through additions and alterations. There comes a point when this growth results in failure to meet one or more criterion, and restrictions on the allowable use of consumable fluids, or the vessel's operational envelope are enforced. It is expected that through better understanding of the stability criteria and how they are related to capsize risk, a more rational approach to through-life stability management will be developed. This may be through allowing some criteria to be traded against others to achieve a consistent level of safety or through evaluating the effect of failure to meet particular criterion on capsize risk, allowing a more cost-effective approach.

3 Numerical Simulations

3.1 Background

3.1.1 In 1990 the Cooperative Research Navies (CRNavies) Dynamic Stability group was established with the aim of investigating and deriving dynamic stability criteria for naval vessels. To derive such criteria, the group needed to evaluate in-service and new ship designs, in moderate to extreme seas in terms of their relative safety and probability of capsize. This would ensure that new vessels continued to be safe, while avoiding high build and life-cycle costs associated with over-engineering.

3.1.2 To achieve these objectives the numerical simulation program FREDYN was developed, and continues to be applied extensively – both to intact and damaged ships. This time-domain program is able to take account of nonlinearities associated with drag forces, wave excitation forces, large-angle rigid-body dynamics and motion control devices. The FREDYN program permits investigations into the dynamics of intact and damaged vessels operating in realistic environments.

3.1.3 Recent work within the CRNavies group has involved the investigation of existing stability criteria parameters as a function of a short term Critical Roll Index using a probabilistic approach developed by the CRNavies group. Comparisons have been made between the short term and annual Critical Roll Index results produced for the candidate frigates for the CRNavies.

3.1.4 These studies have shown the current naval static stability criteria terms which are key indicators of the intact dynamic stability performance of the vessel. This methodology was used for this project, in order to evaluate the dynamic stability performance of three passenger vessels and relate that to the current static stability criteria.

3.1.5 By using a conventional vessel that satisfactorily passes the current stability criteria, it allows the dynamic performance in realistic wind and waves to be evaluated and compared to the more unconventional hull forms. This performance can also be related back to static stability criteria terms, which identifies the individual terms and the levels that will give the equivalent level of stability performance. It also indicates which criteria terms provide the best indication of the dynamic stability performance.

3.2 Test Vessels for the Study

3.2.1 In consultation with the MCA, three vessels were selected for the numerical study. The first is a more conventional vessel, the MV ST. OLA, which complies with all the stability requirements of the IS code, with maximum GZ occurring at a heel angle in excess of 30 degrees. The two other vessels that were selected were of similar size and pass the IS code apart from maximum GZ occurring at heel angles just below 25 degrees. These vessels are the MV HEBRIDES and MV LORD OF THE ISLES. The main dimensions are given below in Table 3-1.

Ship Name		MV ST. OLA	MV HEBRIDES	MV LORD OF THE ISLES
Length BP	[m]	79.45	91.2	75
Breadth Moulded	[m]	16.3	15.8	15.8
Draught Amidships	[m]	3.95	3.21	3.1
Cb	[-]	0.59	0.74	0.64
Displacement	[Te]	3100	3491	2398
Trim	[m]	0.04	0.16	0.05
LCG fwd AP	[m]	37.1	44.09	36.22

Table 3-1 – 3 Test Vessels

3.3 FREDYN – Non Linear Time Domain Program

3.3.1 The time domain program FREDYN was used for all the numerical simulations and calculations of a critical roll index (probability of exceeding a set roll angle). The program has been extensively validated for a variety of ship types. However, further validation was conducted as part of this project by undertaking scale model tests with one of the chosen ferries. These results are presented in Section 4.

3.3.2 FREDYN is a time domain code which solves equations of motion in six degrees of freedom. The code operates by combining viscous forces and potential forces to complete the physical model, and is able to account for non-linearities associated with drag forces, excitation forces and rigid body dynamics. A physical approach is used in which all physical factors affecting the ship can be considered.

3.3.3 It is important that a code which can account for non-linearities is used when investigating large roll angles because these arise from:

- The effect of large angles on excitation forces.
- The effect of large angles on rigid body dynamics.
- Drag forces associated with hull motions, wave orbital velocities and wind.
- Integration of wave induced pressure up to the free surface.

The use of FREDYN allows realistic investigations into dynamic stability in realistic environments, rather than the simple pseudo-static analysis currently used.

3.4 Probabilistic Calculation of Critical Roll Index

3.4.1 FREDYN simulations were used to evaluate the critical roll (capsize) behaviour of the three vessels in a range of loading conditions from passing the IS code through to failing. This Critical Roll Index Parameter allows the dynamic performance to be compared with the static stability criteria parameters.

3.4.2 It is understood that a capsize risk value produced by simulations has, in isolation, limited true meaning and should not be taken as an absolute level of capsize risk. The risk value produced by the simulations is therefore described as a Critical Roll Index rather than a pure capsize risk. For this study a roll angle of 45 degrees was selected as the critical roll angle, based on the vessel's ranges of positive stability. For naval vessels an angle of 70 degrees is typically used as the critical roll angle, as it is the downflooding angle often assumed. The capsize risk index values (taken as 45 degrees roll in this study) are, however, a good measure of dynamic stability that can be used to compare different vessels(or the same vessel at several loading conditions) at different headings, environmental conditions and static stability values.

3.4.3 The methodology used to calculate the Critical Roll Index is similar to that used by QinetiQ within the CRNavies group to determine a Critical Roll Index for naval vessels and relate that to the current static stability criteria. This procedure was developed by McTaggart [32] in 2002 and is described further in his paper [37]. A conventional vessel which passes current stability standards with acceptable performance is tested as a benchmark. This vessel's Critical Roll index can then be compared to the more unconventional vessels which have the low peaking GZ max angles. The relationship between the static criteria terms and the affect on the dynamic performance on the vessels (i.e. critical roll index) can then be calculated and suitable levels to maintain an equivalent level of dynamic stability and hence capsize safety can be identified.

3.4.4 The method used to determine the critical roll index combines predictions from FREDYN with probabilistic input data for wave conditions and ship speed and heading. The probability of capsize C_D in a random seaway of duration D is thus [32]:

$$P(C_D) = \sum_{i=1}^{N_{V_s}} \sum_{j=1}^{N_\beta} \sum_{k=1}^{N_{H_s}} \sum_{l=1}^{N_{T_p}} P_{v_s}(v_{s,i})\, P_\beta(\beta_j)\, P_{H_s,T_p}(H_{s,k} T_{p,l})\, P(C_D \mid V_s, \beta, H_s, T_p) \qquad (1)$$

where:

V_s = ship speed

β = wave heading relative to ship

H_s = wave significant height

T_p = wave modal period

3.4.5 The last term is a conditional probability of capsize in a given wave condition and ship course. The method does not take account of the influence of the operator. That is, situations such as higher-speed running in stern quartering seas, which would generally be avoided, are considered equally probable as safer modes of operation. It is also assumed that propeller revolutions required to maintain a given speed in calm water were also set in waves. For this study only two suitable speeds were selected to avoid unrealistic operator speed decisions, although an even probability of heading was assumed.

3.4.6 Using this method the dynamic behaviour of the vessel was simulated at every speed and heading combination at a wide range of significant wave heights and modal wave period combination. Up to 30 simulations were conducted at each speed/heading/wave condition to generate data to calculate the probability of reaching the critical roll limit. A Bales wave climate statistics table [36] for the North Atlantic was used to provide the probability of the waves occurring. This has been used for previous studies [32][34] and was used for all test ships in this study so a direct comparison can be made. For this study both the full and cut down wave scatter tables were used. The cut down wave scatter table was limited to a maximum of mid sea state 7, so the vessels performance in the very extreme waves could be removed from the analysis. A sea state 7 is still considered extreme seas for these vessels.

3.4.7 The probability of capsize, based on sumilation durations of 1 hour, has been computed using equation 1. Originally the associated annual probability of capsize was calculated from the following equation:

$$P(C_{annual}) = 1 - [1 - P(C_D)]^{\alpha \times 1\,year/D} \quad (2)$$

Where α is the fraction of time spent at sea and D is duration. QinetiQ moved to use the 1 hour short term risk values as indications of the vessel's dynamic performance as this gave a better indication of performance than the annual results. This method of analysis has been implemented into a suite of software codes [32].

3.4.8 Previous studies conducted using this method have used three ship speeds for the probabilistic calculations which is simple, but is not vessel specific and has no operator influence [32][34]. However, this was shown to produce unrealistically high Critical Roll index (capsize probability), due to the large speed envelope for the vessels tested and was shown to be unreasonable, particularly for the smaller vessels. For previous studies with a smaller 56m naval vessel, speeds of 10 and 12 knots were used. These were chosen after discussions with the naval operators and an interactive investigation with FREDYN. This identified the most realistic speed choice that would be made for the smaller vessels so as to keep control as the waves increased in size. Simulations at slower speeds showed a loss of steerage and consequently a heading change into beam seas, which resulted in large roll angles and an unrealistically high Critical Roll Index (capsize risk probability).

3.4.9 For this study the FREDYN simulations were completed for each ship in three different loading conditions. The simulations covered a range of headings from 0° (head seas) to 180° (stern seas) in 30° increments. The speed profile for each ship was simplified so that all ships were tested at the same speeds of 8 and 12 knots. These speeds were selected as being realistic for vessels of their size, based on their speed envelope.

3.4.10 A Bretschnieder spectrum was used to simulate the wave conditions typically found in the North Atlantic. Wind forces were also included collinear with wave direction, and the mean wind speed related to wave height using the following expression [32]:

$$\overline{V_w} = 1.823 H_s + 3.45 \quad (\text{m/s})$$

where:

$\overline{V}_w$ = mean wind speed

3.4.11 Distribution curves were used to fit to the calculated peak roll angle data from each hour length simulation in each of the seaway conditions. McTaggart [32] found that Limited Gumbel distribution and a Distribution free method produced the best results from his extensive study [32].

3.4.12 The limited Gumbel distributions and the distribution free curves provided the best data fit and better prediction at the higher roll angles which were of the most interest for critical roll (capsize) prediction [32]. The Gumbel distribution has the advantage that it can be used to extrapolate beyond the observed range of values. The distribution free predictions have less bias associated with them than using fitted distributions [32]. As the critical roll angle in this study was set to 45 degrees, the distribution free curve was used to fit to the roll data. A small selection of terms were calculated using the Gumbel distribution and a 70 degree critical roll angle for comparison of the trends of relative capsize risk.

3.4.13 The fit used the upper 30 degree range of the simulation and fits to a minimum of 10 data points. These methods were validated on large numbers of simulations (400+) by McTaggart. However this number of runs was not feasible for routine calculations, as the time to compute would be months. Realistically the number of simulations had to be between 10 and 50. The sensitivity of using this number of runs was investigated and showed to give very good results with a maximum of 30 runs [32].

3.4.14 The process described above was repeated for each vessel in each condition to determine the most important criteria in assessing dynamic stability.

3.4.15 Each ship load condition combination required approximately 800 computer processor hours to complete.

3.5 Computational Model Setup and Load Conditioning

3.5.1 A model of each ship was created in the PARAMARINE design software. Lines data for MV ST. OLA were taken from a SIKOB model supplied by MCA. Appendages, profiles and superstructure details were taken from archive drawings [26] to [31]. PARAMARINE models of MV HEBRIDES and MV LORD OF THE ISLES were generated from IGES surfaces supplied by Alder Marine Consultants via the MCA. A selection of images created from PARAMARINE can be found in Annex A.1. The models were validated against the supplied hydrostatic data.

3.5.2 Three loading conditions were defined for each model. One condition was chosen to match the limiting condition according to the IS Code, allowing an assessment of the current level of performance afforded by these regulations. Two alternative conditions were also tested with one having a higher GM, based on a typical loaded arrival operating condition, and one having a lower GM. Thus, one alternative conditions failed the IS Code criteria and the other passed by some margin. The displacement and trim in each condition were identical and set to match that of the loaded arrival condition. Table 3-2 details the loading conditions tested for each ship. As the exact mass distribution of the ships was not known the radii of gyration were estimated using the following approximations:

$$K_{YY} = K_{ZZ} = 0.24L$$
$$K_{YY} = 0.3B$$

Ship Name		MV ST OLA			MV HEBRIDES			MV LORD OF THE ISLES		
Length between Perps	[m]	79.45			91.2			75		
Breadth Moulded	[m]	16.3			15.8			15.8		
Draught Amidships	[m]	3.95			3.21			3.1		
Cb	[-]	0.59			0.74			0.64		
Displacement	[Te]	3100.9			3491.4			2398.3		
Trim	[m]	0.04			0.16			0.05		
LCG fwd AP	[m]	37.1			44.09			36.22		
Condition		**1**	**2**	**3**	**1**	**2**	**3**	**1**	**2**	**3**
KM	[m]	8.59	8.59	8.59	8.58	8.58	8.58	9.48	9.48	9.48
KG	[m]	7.26	7.83	8.13	7.15	7.45	7.75	6.91	7.13	7.34
GM	[m]	1.33	0.76	0.46	1.43	1.13	0.83	2.57	2.35	2.14
$K_{YY} = K_{ZZ}$	[m]	17.88	17.88	17.88	20.52	20.52	20.52	16.88	16.88	16.88
K_{XX}	[m]	4.89	4.89	4.89	4.74	4.74	4.74	4.74	4.74	4.74
IS Code Criteria										
A_{30}	[m-rad]	0.18	0.10	0.06	0.21	0.16	0.12	0.25	0.22	0.19
A_{40}	[m-rad]	0.28	0.15	0.08	0.28	0.21	0.14	0.36	0.31	0.26
A_{30-40}	[m-rad]	0.11	0.05	0.02	0.07	0.04	0.01	0.10	0.08	0.06
Max GZ angle	[deg]	44.00	30.00	25.00	25.00	24.00	23.00	26.00	25.00	24.00
Max GZ above 30°	[m]	0.64	0.30	0.15	0.57	0.42	0.27	0.69	0.58	0.47
Weather Criterion a/b	[-]	1.64	0.53	*	1.06	0.78	0.51	1.22	0.99	0.78

a/b for 25 degree roll back angle, * = Lw2 > GZ_{max}

Table 3-2 Ship GZ Parameters

3.5.3 Figure 3-1, shows the GZ curves calculated by PARAMARINE for MV ST. OLA in the following conditions:

a. The actual operational condition at the loaded arrival state.

b. The maximum KG allowed according to the IS-Code for the displacement and trim of (a).

c. KG outside the limit of the IS-Code at the same displacement and trim as (a).

For comparison, the calculated curve for condition a. is compared to that extracted from the ship's stability book.

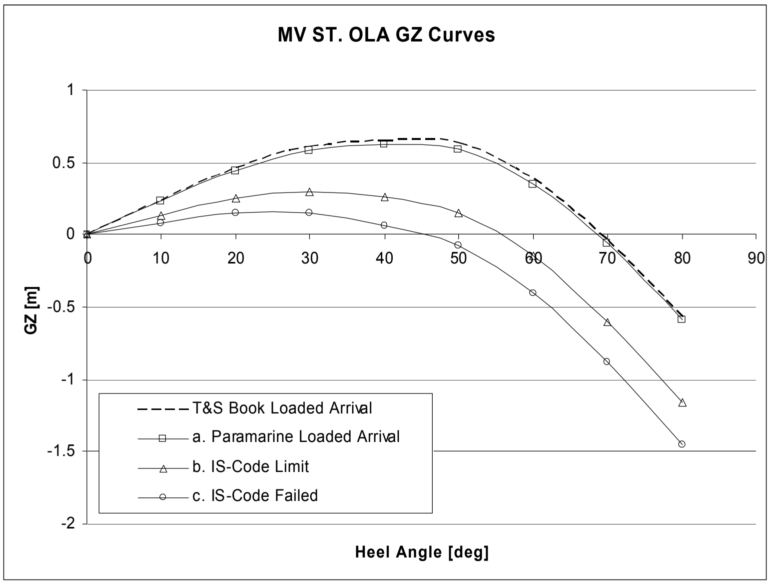

Figure 3-1 MV ST. OLA GZ Curves

3.5.4 The GZ curves for the 3 vessels calculated by PARAMARINE in the 3 loading conditions are shown below in Figure 3-2.

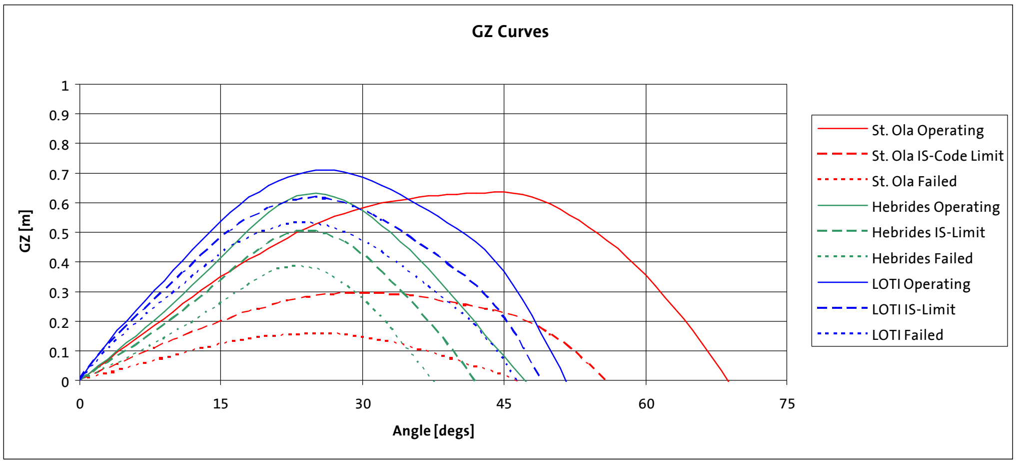

Figure 3-2 – GZ Curves for the 3 vessels at 3 loading conditions

3.5.5 Routines within PARAMARINE were used to determine the GZ criteria to subsequently compare with Critical Roll Index (see Section 6). A dedicated FREDYN export tool was used to generate FREDYN hull definitions and input files for each condition.

3.5.6 FREDYN simulations were performed in identical wave conditions for each ship and condition so as to compare each ship on the same basis. The same operating profile was assumed for all three ships.

Blank Page

4 Model Tests

4.1 Introduction

4.1.1 The FREDYN program was selected for the numerical investigations in this study due to its ability to simulate the motions of a ship in moderate to extreme waves. The FREDYN program has been continually validated and improved over the last 18 years for naval hullforms by the CRNavies working Group, much of which is not available in open literature.

4.1.2 FREDYN has been previously compared successfully with experiment data for a number of commercial vessel types as well as numerous naval hullforms. As the vessels involved in this study are still relatively conventional mono-hulls, there is nothing to suggest that FREDYN is not capable of adequately predicting the motions of these vessels in moderate to extreme waves. In order to provide additional validation and comparison with the FREDYN simulation predictions, a limited series of model tests in beam sea waves were conducted in the Ship Tank at QinetiQ Haslar. The model was very lightly tethered to ensure it remained in beam seas, although the tendency of the model to yaw was not found to be great.

4.1.3 In consultation with the MCA, the conventional vessel for use in this investigation was selected as the MV ST. OLA, which was also tested in the numerical capsize risk study. The vessel and scale model properties are displayed in Table 4-1 below:

Scale ratio 1:30		Model		Ship equivalent	
		Operating	IS-Code Limit	Operating	IS-Code Limit
Length BP	[m]	2.648		79.45	
Beam	[m]	0.543		16.30	
Draught	[m]	0.132		3.95	
Displacement	[Te]	0.112		3101	
Trim	[m]	0.001		0.04	
LCG fwd AP	[m]	1.237		37.1	
KM	[m]	0.287	0.287	8.61	8.61
KG	[m]	0.242	0.261	7.26	7.83
GM	[m]	0.045	0.026	1.35	0.78
Roll Period	[s]	1.79	2.32	9.8	12.7
K_{ZZ}	[m]	0.636	0.636	19.08	19.08
K_{ZZ}/L_{PP}	[-]	0.240	0.240	0.24	0.24

Table 4-1 Physical Model Properties

4.2 Model Construction

4.2.1 A 1:30 scale model of MV ST. OLA was constructed from foam and fitted with accurately scaled appendages, including propellers which were locked in position. The model was fitted with a simple representative foam superstructure to prevent inversion in the event of capsize. The bilge keel span was only 8mm at its maximum point on this 3m model.

4.3 Model Instrumentation

4.3.1 A Crossbow Inertial Reference Unit (IRU) unit was installed to measure roll, pitch, heave acceleration and heading. A light, flexible umbilical exited the model through a gland to transfer data to the acquisition system that was positioned on the ship tank carriage. One 2-sword resistance type probe and one ultrasonic wave probe were used to measure wave elevation as experienced by the model. Calibration limits, accuracy and pre/post experiment linearity are detailed in Table 4-2.

		Range	Pre-Experiment Calibration Factor	Pre-Experiment Max Uncertainty	Post-Experiment Calibration Factor	Post-Experiment Max Uncertainty	Calibration Drift
Tank RW Wave Probe	[mm]	± 30 mm	-16.11	3.0%	-15.74	3.0%	-2%
Carriage US Wave Probe	[mm]	± 30 mm	-0.05	2.5%	-0.05	3.0%	1%
Carriage RW Wave Probe	[mm]	± 30 mm	0.10	0.6%	0.10	0.4%	0%
Heading	[deg]	± 180°	43.64	3.0%	Check cals conducted - all valid		
Roll	[deg]	± 90°	11.08	0.6%	11.06	0.7%	0%
Pitch	[deg]	± 45°	-8.81	0.5%	-8.82	0.7%	0%
Heave Acceleration	[m/s²]	± 9.81 m/s²	1.19	0.1%	1.19	0.9%	0%

Table 4-2 Calibration Factors

4.4 Model Conditioning

4.4.1 The model was ballasted to one displacement and trim only. Ballast was adjustable vertically to achieve two different vertical centre of gravity (VCG) heights. The longitudinal centre of gravity (LCG), roll period and pitch gyradius were set to the required values in the lower VCG condition. The yaw gyradius was assumed equal to pitch gyradius which is standard model conditioning practice for conventional monohulls. The longitudinal weight distribution was unaffected by the adjustment in VCG; this was confirmed by measuring pitch gyradius in both conditions. The natural roll period in each load condition was measured and roll decay tests were recorded. The roll gyradius of the numerical model was then adjusted accordingly to match the experiment model. The weights used for ballasting were fixed in place due to the large roll angles expected.

4.4.2 Transformation between the two conditions was achieved by moving two weights from deck level inside the model to recesses cut into the bottom of the foam superstructure. To enable fine adjustment of LCG and VCG a single 2.2kg mass was fixed to the top of the superstructure. This weight was included when calculating other parameters and required only a small (25 mm) lateral adjustment to achieve the final trim. Table 4-1 above details the achieved model parameters, including instrumentation and all ballast masses, and their ship scale equivalents.

4.5 Test Programme

4.5.1 The model tests were performed at zero speed in beam seas. Due to the time and cost which would be involved with a comprehensive set of free-manoeuvring model experiments only a limited series were conducted to validate the FREDYN simulations. As the aim of the study was to predict and compare large roll angles the model tests were performed in a range of wave conditions.

4.6 Roll Decay Tests

4.6.1 With the model in each load condition a number of roll decay tests were performed to determine calm water roll damping, ensuring consistency between the FREDYN model and actual experimental data. The weight distribution in the FREDYN model was adjusted so that the GM, displacement and natural roll period matched that of the experiment model.

4.7 Regular Wave Tests

4.7.1 Prior to the experiments the wavemakers were calibrated using the wave probes to ensure the set wave height and period matched that measured. The large regular waves were measured and the numerical model waves were adjusted to match those measured at the model.

4.7.2 A wave probe was mounted to the ship tank at the model starting position to acquire wave data during the run. A second sonic wave probe was also positioned in line with the model off to one side to measure the waves the model encountered.

4.7.3 Each run was started with the model at zero speed, beam on to the wavemakers with a separation of approximately 30 m. Light restraining lines were attached for emergency control and to return the model to its starting position after each run. The wavemakers were started, and data collection began after the waves achieved a steady state. The ship tank carriage speed was adjusted to match the model's drift. The acquisition period was carefully controlled to minimise the effect of waves reflected from the far end of the tank.

4.7.4 Wave period was calculated by deriving a power spectrum of wave elevation using Welch's averaged modified periodogram method. The wave period was taken as that of the peak spectral ordinate (i.e. the modal period). Note that wave period was taken from the tank-fixed wave probe as the carriage-fixed probe was sensitive to the effects of drift on encounter frequency. The peak-peak wave amplitude was also calculated from the area bounded by the power spectrum.

4.7.5 Table 4-3 below details the demanded and measured regular wave properties.

4.8 Irregular Wave Tests

4.8.1 As with the regular wave tests, the irregular wave tests began with the model beam on to the oncoming waves. The wavemakers were calibrated before the tests to ensure the full range of frequency components were generated and experienced by the model and that the correct significant height was being generated. A ramp-up period was allowed between starting the wavemakers and recording data. Power Spectral Density (PSD) plots (i.e. wave energy spectra) were derived using Welch's averaged, modified periodogram method with a default Hamming window and 50% overlap.

4.8.2 Significant wave height was calculated according to Lloyd [33]:

$$H_s = 4\sqrt{\int_0^{\infty} S_\zeta(\omega)\, d\omega}$$

where:

H_s = significant wave height (m)

S_ζ = wave height spectral ordinate (m^2/(rad/sec))

ω = wave frequency (rad/sec)

4.8.3 To avoid the effects of high frequency noise on this derived significant wave height the data were filtered using a low-pass filter set at 2 Hz prior to acquisition.

4.8.4 Mean period and modal period of the waves were calculated from the derived spectrum; mean period is found by taking moments of spectral area about the y-axis and modal period is the reciprocal of modal frequency. Details of the irregular waves set are included as part of Table 4-3.

	Wave Set	Demanded Period [s]	Demanded Amplitude (peak-peak) [m]	Measured Period [s]	Measured Amplitude (peak-peak) [m]
Condition 1	Regular 1	8	2.5	7.98	2.40
	Regular 2	9	2.5	9.01	2.68
	Regular 3	10	2.5	10.02	2.04
	Regular 4	11	2.5	11.00	2.31
	Regular 5	12	2.5	12.00	2.52
	Regular 6	14	2.5	14.02	2.59
	Capsize 1	12	3.5	12.00	3.59
	Capsize 2	10	4.5	10.02	4.48
	Capsize 3	10	5.5	9.97	5.69
	Capsize 4	10	6.5	10.02	6.20
	Capsize 5	10	7.5	10.02	7.75
	Irreg 1	8.8	1.88	8.63	1.88
	Irreg 2	12.4	5	12.2	5.71
Condition 2	Regular 1	10	2.5	10.02	2.24
	Regular 2	12	2.5	12.00	2.53
	Regular 3	13	2.5	13.04	2.50
	Regular 4	13.5	2.5	13.51	2.42
	Regular 5	14	2.5	14.02	2.59
	Regular 6	15	2.5	14.96	2.73
	Capsize 1	13	4.5	13.04	4.48
	Capsize 2	13	6.5	13.04	6.55
	Capsize 3	13	8.5	13.04	8.62
	Capsize 4	13	10.5	13.04	12.91
	Capsize 5	11	10	11.00	10.08
	Irreg 1	8.8	1.88	8.63	1.90
	Irreg 2	12.4	5	11.9	5.38

Table -4-3 Wave Details

4.8.5 The original model test specification stated that 2 KG conditions, 4 irregular waves and 3 regular waves would be tested. It was found more beneficial for the validation to run a greater set of regular waves (6 standard and 5 large regular waves) and reduce the irregular waves to 2 (sea states 4 and 6).

5 Comparison of Model Experiments with FREDYN Simulations

5.1 Introduction

5.1.1 A limited series of model tests were performed to support the capsize predictions made using the FREDYN program. Predictions in regular and irregular waves were compared to experimental data to assess the predictions of FREDYN for the hullforms used.

5.1.2 Roll decay comparisons were initially conducted to compare the roll damping between the experiment and the numerical simulations. While it is possible to tune the damping coefficients within the FREDYN program to achieve a near match to the experiments, this was avoided as measured decay data was not available for the other test vessels that were to be calculated in the numerical study. The FREDYN predictions were, therefore, produced using the standard damping calculations based on hullform and appendages dimensions only. A comparison of the roll decay for the operating condition is shown in Figure 5-1.

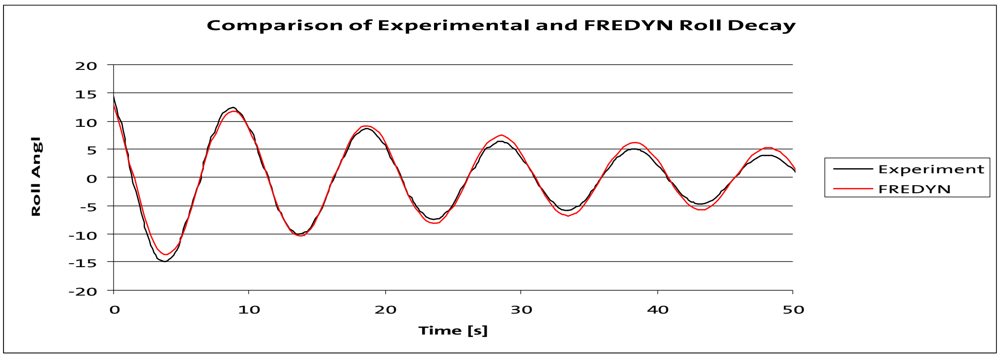

Figure 5-1 – Roll Decay Curve for St OLA experiment and FREDYN simulation (Operating Condition)

5.2 Wave Details

5.2.1 Due to the different methods of generating irregular time histories between FREDYN and the ship tank wavemaker software, the irregular wave time histories generated by the two methods were not identical. However, statistically they were near identical so it was acceptable to compare the statistics of the resulting motions (i.e. RMS motions). Regular waves were consistent between FREDYN and the model tests.

5.3 Regular Wave Induced Motions (small waves)

5.3.1 The wave amplitude varies slightly between each run through natural experimental variation, and so it is appropriate to normalise the roll response against wave slope. It is then possible to report the non dimensional amplitude at the appropriate wave frequency, i.e. the Response Amplitude Operator (RAO). The wave slope amplitude is calculated according to Lloyd [33]:

$$\alpha_0 = \frac{\pi H}{\lambda}$$

where

H = wave height (peak – peak) calculated from 2√2 RMS of the wave trace.

λ = wavelength.

Motion RMS values and amplitudes are determined from the motion traces and used to calculate RAOs. The RMS values are used to take account of the small variations in wave height, which is due to a well known "beat" phenomenon in towing tanks. The RAO is calculated by:

$$RAO_{\text{Displacement}} = \frac{\text{RMS displacement}}{\text{RMS wave amplitude}} \qquad RAO_{\text{Angle}} = \frac{\text{Angular motion amplitude}}{\text{wave slope amplitude}}$$

5.3.2 Motion phase angles were calculated by determining the RMS error between the wave and motion traces. The phase response was determined from the phase shift which produced the minimum RMS error. The phase is therefore derived from the phase shift required to reach the phase angle at which the normalised wave and motion traces are most closely matched.

5.3.3 Table 5-1 details values of the roll RAOs in regular waves calculated from FREDYN and using model test data.

Regular Waves			
	Frequency [Hz]	FREDYN RAO [-]	Model Test RAO [-]
Operational	0.125	0.99	0.93
	0.111	2.79	2.90
	0.100	5.77	6.53
	0.091	3.64	3.61
	0.083	2.41	2.04
	0.071	1.68	1.39
IS-Code Limit	0.100	0.61	1.16
	0.083	3.31	3.75
	0.077	4.83	6.88
	0.074	3.57	6.14
	0.071	2.68	3.43
	0.067	1.94	2.36

Table 5-1 FREDYN Validation in Regular Waves

5.3.4 Figure 5-2 and 5-3 below show the roll RAO curves in regular waves calculated from FREDYN and those calculated using the model test data. The roll phase response is also plotted for comparison.

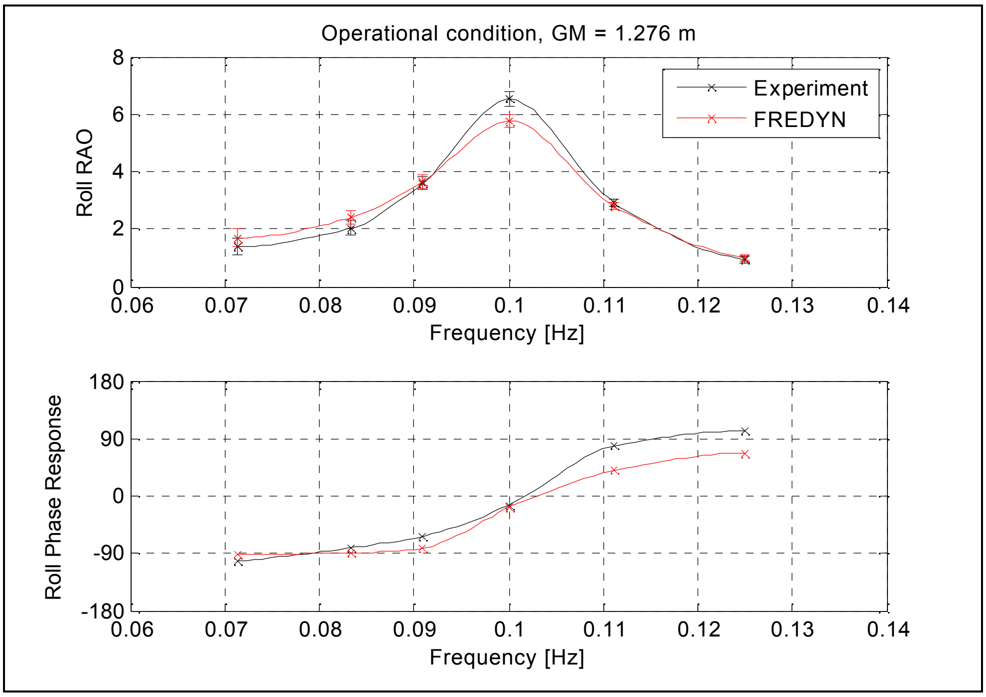

Figure 5-2 – MV St Ola Operating Condition – Experiment and FREDYN RAO

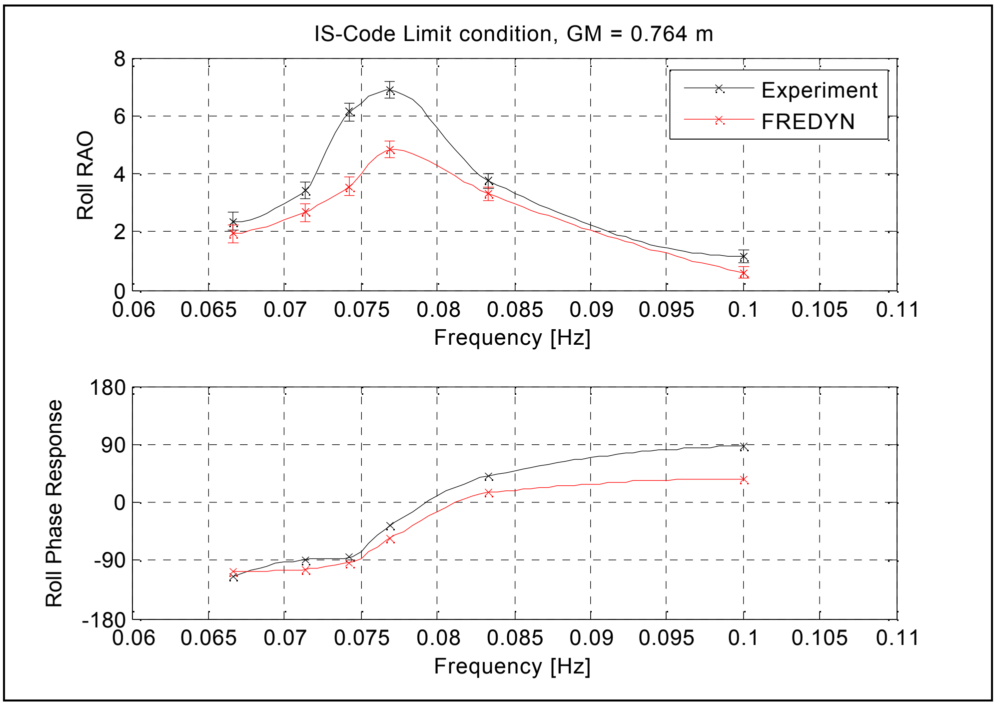

Figure 5-3 – MV St Ola IS Code Limit – Experiment and FREDYN RAO

5.3.5 Experimental data is always subject to physical error so error bands have been calculated and included on the Figures above. In regular waves the wave profile differs slightly from a perfect sine wave. Variations in wave profile from ideal sine waves are small, and their effect is considered negligible. Variations in amplitude have greater effect, and can be significant, for example, in the large amplitude regular waves. Percentage error is derived from the variation in peak values divided by the mean peak value. The error band used includes the influence of both wave and motion amplitudes.

5.3.6 Figure 5-1 shows a close comparison between the experiment results and the FREDYN simulations for MV ST OLA's operating condition. The IS limiting case, Figure 5.2, shows the correct trend but the peak of the curve in FREDYN is lower than the experiment, suggesting FREDYN has greater damping than the experiment. The loading condition is the only change between the two conditions. The difference could be due to the longer roll period (due to the lower GM) leading to some damping issues with the experiment, such as some laminar flow effects at this slower roll. This could be due to the small bilge keels on this vessel, which on the 3m model are very small (<8mm outreach- see Figs B1 and B2 in Annex B). These effects may not occur at the faster roll rates, hence the results are close at the lower wave periods.

5.4 Regular Wave Induced Motions (Steep waves)

5.4.1 Table 5-2 compares the maximum roll angles predicted by FREDYN and those recorded during the model tests in the large and steep waves. In these conditions there is the added complexity since the appendages such as bilge keels and rudders are emerging from the water at the large roll angles, significantly affecting the model roll damping.

	Wave Period [s]	Peak-Peak Height [m]	Experimental Accuracy [Error Band]	Roll Max Experiment [deg]	Roll Max FREDYN [deg]	Difference [%]
Operational	12.00	3.61	5.4%	6.54	7.27	-11.16
	9.99	3.77	13.4%	24.64	22.57	8.40
	9.99	4.83	13.4%	26.12	24.60	5.82
	9.99	5.21	12.2%	27.71	26.03	6.06
	9.99	6.52	11.8%	30.16	29.46	2.32
IS-Code Limit	13.01	4.5	6.2%	18.98	14.77	22.18
	13.01	6.56	6.7%	24.37	19.66	19.33
	13.01	8.64	7.6%	27.49	22.03	19.86
	13.04	9.42	12.9%	30.51	23.70	22.32
	11.00	9.46	17.9%	23.55	23.85	-1.27

Table 5-2 – MV St Ola – Experiment and FREDYN Maximum roll angles

5.4.2 As in the shallower wave comparison, the difference between the experiment and the simulation is relatively small in the operational condition, demonstrated by several results better than 8% error. The IS limit loading condition again shows some increased differences at the slightly longer wave period, where the shorter 11 second wave period case is within 2% of the experiment.

5.5 Irregular Waves

5.5.1 Two sets of irregular waves were physically tested for each load condition; mid sea states 4 and 6. The test waves were also run in the FREDYN simulation. Although the same sea states were tested, different random phase angles were used to generate the time history as FREDYN and the ship tank wavemakers use different algorithms to compute these angles. RMS roll motion amplitudes may be legitimately compared when there are at least 100 wave encounters, despite these differences in wave time histories. Due to the scale of the model the largest sea state that could be modelled was a mean sea state 6.

5.5.2 The comparison between the experiment and FREDYN simulations are shown below in Table 5-3.

		Experiment RMS [degs]	FREDYN RMS [degs]	Difference RMS [degs]	% Difference RMS
Operating	Sea State 4 (JS)	4.16	4.38	-0.22	5.3%
	Sea State 6 (JS)	7.06	7.69	-0.63	8.9%
IS-Code Limit	Sea State 4 (JS)	0.99	0.74	0.25	-25.6%
	Sea State 6 (JS)	5.64	5.25	0.39	-7.0%

Table 5-3 – RMS Roll Angle comparisons between experiment and simulation

5.5.3 The comparison between the experiment and FREDYN simulations in the operating condition show that FREDYN is calculating the RMS roll better than 0.63 degrees in the largest sea state 6 conditions tested. This equates to a percentage difference of 8.9%. The limiting case shows a large percentage difference in the sea state 4 case, due to the very small roll motion that was measured in both experiment and simulation. In the larger sea state 6 waves where there was greater roll motion, the simulation and experiment agree within 0.39 degs RMS, which equates to a 7% difference.

Blank Page

6 Critical Roll Index and Static Stability Criteria

6.1 Introduction

6.1.1 The Critical Roll Index values produced by current ship simulations should not be taken as an absolute level of capsize risk for the vessel. The critical roll index values calculated for this study are, however, a good measure of the dynamic stability performance of the vessels. They allow comparison to be undertaken between the load conditions, headings, environmental conditions and with the static stability terms.

6.1.2 As with previous studies [34] plotting the critical roll index at a range of loading conditions against the corresponding static stability terms give an indication of the current static stability terms that give the best indication and relationship with the dynamic stability performance. This allowed the current criteria to be ranked, which gave the best indication of dynamic stability performance. By comparing the whole set of criteria it was possible to get an indication of the relative level of dynamic stability performance associated with meeting each of the stability criteria terms.

6.1.3 It has been found in previous studies [34], that plotting the capsize risk on a logarithmic scale showed improved trends over the standard linear scale used in previous studies. In this and previous studies both exponential and power curve trend lines have been fitted to the plots of stability criteria and critical roll index and produced some close relationships.

6.2 Static GZ Criteria

6.2.1 In addition to the GZ criteria covered by the IS Code, a number of further parameters of the GZ curves were extracted. These criteria and their values were calculated by PARAMARINE and summarised for each of the three ships tested in Table 6-1.

6.2.2 Due to the unavailability of certain data required to accurately determine the roll to windward due to the waves for the a/b weather criterion value for each of the vessels conditions, the value of 25 degrees was used. The calculations for the IS code are based on data from vessels with a B/T of less than 3.5. The three vessels tested have B/T ratios outside of these data parameters. This 25 degree roll assumption was based on a number of calculations using approximated data for the 3 vessels which resulted in values around 25 degrees. This value was set the same for all the conditions and vessels tested. The similar naval vessel criteria also use a set value of 25 degrees.

		St. Ola			Hebrides			Lord of the Isles		
		Loaded Arrival	IS-Code Limit	Failed IS-Code	Loaded Arrival	IS-Code Limit	Failed IS-Code	Loaded Arrival	IS-Code Limit	Failed IS-Code
Displacement	[Te]	3100.9	3100.9	3100.9	3491.4	3491.4	3491.4	2398.3	2398.3	2398.3
Cvp	[-]	0.71	0.71	0.71	0.796	0.796	0.796	0.737	0.737	0.737
GMt	[m]	1.341	0.766	0.467	1.426	1.126	0.827	2.569	2.346	2.14
Area to 15°	[m-rad]	0.049	0.028	0.017	0.055	0.044	0.033	0.079	0.071	0.063
Area to 20°	[m-rad]	0.085	0.048	0.029	0.100	0.085	0.062	0.132	0.118	0.105
Area to 25°	[m-rad]	0.1281	0.0721	0.043	0.1533	0.124	0.0949	0.128	0.1712	0.1511
Area to Gmax	[m-rad]	0.3286	0.098	0.043	0.1533	0.1152	0.0816	0.2052	0.1712	0.1418
Area to 30°	[m-rad]	0.177	0.098	0.056	0.206	0.164	0.123	0.254	0.223	0.195
Area to 40°	[m-rad]	0.284	0.147	0.075	0.279	0.207	0.135	0.358	0.305	0.256
Total area	[m-rad]	0.502	0.191	0.078	0.293	0.208	0.139	0.416	0.336	0.268
Area 30°-40°	[m-rad]	0.107	0.049	0.019	0.073	0.043	0.012	0.104	0.082	0.061
Area 15°-rps	[m-rad]	0.453	0.163	0.061	0.238	0.163	0.106	0.337	0.265	0.205
Area 30°-rps	[m-rad]	0.325	0.093	0.022	0.087	0.043	0.016	0.162	0.112	0.074
Area 40°-rps	[m-rad]	0.218	0.045	0.003	0.015	0.001	0.000	0.057	0.030	0.013
Range Positive Stability	Degs	68.000	55.000	46.000	47.000	41.000	37.000	51.000	47.000	46.000
Total Area/Cvp	[m-rad]	0.7	0.3	0.1	0.4	0.3	0.2	0.564	0.455	0.364
Area 30+/Cvp	[m-rad]	0.457	0.132	0.027	0.110	0.046	0.020	0.219	0.152	0.100
Area 40+/Cvp	[m-rad]	0.218	0.045	0.003	0.015	0.001	0.000	0.057	0.030	0.013
a/b (25 deg)	[-]	1.637	0.528	*	1.059	0.781	0.51	1.216	0.987	0.777
GZMax	[m]	0.636	0.297	0.159	0.630	0.506	0.387	0.711	0.616	0.531
GZMax > 30°	[m]	0.636	0.297	0.147	0.571	0.421	0.271	0.686	0.575	0.472
GZMax Angle	[deg]	44	30	25	25	24	23	26	25	24

a/b for 25 degree roll back angle, * = Lw2 > GZ_{max}

Table 6-1 GZ Parameters

6.3 Influence of GZ Parameters on Capsize Risk

6.3.1 The complete set of Critical Roll Index data from the 3 small domestic passenger vessels was plotted against each of the criteria given in Table 6-1 above. Where applicable a line was marked showing the current static stability criteria limit value. These plots are included in Annex C using all of the data and all of the waves. Annex D includes the same plots using only the data from the two high B/T vessels.

6.3.2 In order to identify which of the static stability criteria terms give the best relationship to the overall dynamic stability performance, two trend lines were fitted to the data sets. The R^2 value was calculated using a least squares fit method, in order to compare and rank the relationship between the Critical Roll Index (capsize probability) data and each of the criteria terms. From the initial data plots in Annex C it was identified that the data followed an exponential / power curve shape in many of the plots and were therefore plotted on a logarithmic scale. Exponential and power fit trend lines were therefore selected for the analysis. The exponential and power fit trend lines used the following equations to fit to the data sets:-

- $y = Ce^{bx}$ where c and b are constants and e is the natural log (Exponential)
- $y = Cx^b$ where c and b are constants (Power curve)

6.3.3 The trend line fitting was conducted on 4 subsets of the data to compare how well the data fitted in each case:-

- The complete data set – 3 vessels and all waves in the wave climate statistics table'

- The two higher B/T vessels – all waves in the wave climate statistics table,

- The complete data set – waves up to mid Sea State 7,
- The two higher B/T vessels – waves up to mid Sea State 7,

6.3.4 The set of figures for all the data with the trend lines are included in Annex C. This set of plots uses the distribution free data fit. The R^2 values were compiled for all four subsets of data and ranked based on how the data fitted to the trend lines.

6.3.5 The R^2 results for the distribution free data fit is included in Table 1 for the exponential trend fit. The results from each subset have then been ranked and the top four criteria terms are highlighted (Gold, Silver, Bronze, dark Bronze). Table 2 provides the fit using a power cure fit and the subsequent ranking.

6.3.6 Comparisons were made between the data sets for all the vessels and the current stability parameters. A selection of the plots were also reproduced using the Gumbel distribution using a greater critical roll angle limit to confirm the relationship between the dynamic performance and the criteria term in Annex C.

Blank Page

7 Critical Roll Index Results Discussion

7.1 Analysis

7.1.1 The Figures in Annex C include data from the three vessels tested, MV St Ola, MV Hebrides and MV Lord of the Isles. It is clear that the logarithmic scale allows trends to be seen in several of the plots. The Figures in Annex D include data from just the two high B/T vessels tested, MV Hebrides and MV Lord of the Isles.

7.1.2 This work assessed the Critical Roll Index (capsize probability measure) associated with the current static stability measures and developed new ways of analysing ship hydrostatics that give the best indication of dynamic stability effects. In previous studies [34], graphs showing the best correlation between ship static stability measures and the probability of capsize (Critical Roll Index) were those relating to the area under the GZ curve. The work during this study builds on this experience in order to improve the understanding of the correlation between ship static hydrostatics and the probability of capsize for higher B/T vessels.

7.1.3 The data that is included in the figures in Annexes C and D was combined and trend lines were fitted to the data as described in Section 6. With closely matching data, the two trend lines fitted to the data produced very similar results. The two tables of the data trend results, ranked by which criteria measures have the closest fit, are copied into this section from Section 12 for clarity.

7.1.4 The difference between the exponential trend fit and the power curve trend fit does not produce widely different R^2 values, as may be expected. Similar trends are also evident in the ranking of the best fitting criteria measures using the two methods.

7.1.5 Table 7-1 and Table 7-2 show the data ranked for the four subsets of data. The top four ranking criteria were colour coded to highlight the criteria with the best data fit. The data set includes the results for all of the vessels in all of the waves tested. There are three further subsets, the second is with all the vessels but with the waves limited to a mid sea state 7. The final two data sets are for the two high B/T vessels in all waves and also restricted to a maximum of a mid sea state 7.

Exponential Parameter	Value All Data All Waves	Value LOTI & Hebrides All Waves	Value All Data Upto Mid SS7	Value LOTI & Hebrides Upto Mid SS7	Rank All Data All Waves	Rank LOTI & Hebrides All Waves	Rank All Data Upto Mid SS7	Rank LOTI & Hebrides Upto Mid SS7
GM_F(m) not less than 0.15	0.3423	0.5129	0.2380	0.1969	17	16	17	15
$AREA_{0-30}$ not less than 0.055	0.5714	0.8717	0.4983	0.5783	10	7	11	6
$AREA_{0-40}$ not less than 0.09	0.7186	0.8825	0.6270	0.5951	8	5	8	5
$AREA_{30-40}$ not less than 0.03	0.8060	0.8956	0.6090	0.6171	5	3	9	3
Area to GZ max	0.9195	0.8375	0.8160	0.5367	2	8	3	9
Angle of GZ_{max} not less than 30	0.3790	0.8864	0.3769	0.6717	16	4	14	4
GZ_{max} not less than 0.2	0.7843	0.9456	0.7438	0.742	6	1	5	2
Total Dynamic Stability	0.9143	0.8081	0.8222	0.5036	3	9	2	10
RPS	0.3825	0.8770	0.3461	0.6134	15	6	16	7
DS/Cvp	0.8840	0.7530	0.7596	0.4308	4	11	4	12
Total Dynamic Stability +30	0.7237	0.7367	0.6622	0.4315	7	12	6	8
DS+30/Cvp	0.6989	0.7037	0.6370	0.3902	9	13	7	11
Total Dynamic Stability +40	0.5414	0.5190	0.5110	0.2353	11	15	10	16
DS+40/Cvp	0.5241	0.4381	0.4939	0.1616	12	17	12	16
Wind A1/A2	0.9634	0.9386	0.9290	0.8352	1	2	1	1
$AREA_{0-15}$ not less than 0.07	0.4659	0.6893	0.3692	0.433	14	14	15	14
$AREA_{0-20}$ not less than 0.065	0.4891	0.7846	0.4022	0.5292	13	10	13	13

Table 7-1 -Exponential fit R^2 values and ranking

7.1.6 The power trend line data and criteria ranking is shown in Table 7-2 below.

POWER Parameter	Value All Data All Waves	Value LOTI & Hebrides All Waves	Value All Data Upto Mid SS7	Value LOTI & Hebrides Upto Mid SS7	Rank All Data All Waves	Rank LOTI & Hebrides All Waves	Rank All Data Upto Mid SS7	Rank LOTI & Hebrides Upto Mid SS7
GM_F(m) not less than 0.15	0.4815	0.6007	0.3843	0.2810	12	15	12	15
$AREA_{0-30}$ not less than 0.055	0.6051	0.9119	0.5521	0.6392	9	5	9	6
$AREA_{0-40}$ not less than 0.09	0.7232	0.9295	0.6606	0.6716	4	4	6	5
$AREA_{30-40}$ not less than 0.03	0.6878	0.9415	0.7058	0.7336	7	3	4	3
Area to GZ max	0.9255	0.9032	0.8605	0.6232	1	6	1	9
Angle of GZ_{max} not less than 30	0.3565	0.898	0.3504	0.6856	14	8	13	4
GZ_{max} not less than 0.2	0.7174	0.9771	0.6884	0.7853	5	2	5	2
Total Dynamic Stability	0.8617	0.8891	0.7831	0.6050	2	11	3	10
RPS	0.4085	0.8908	0.3174	0.6347	13	10	14	7
DS/Cvp	0.8507	0.8954	0.7834	0.5401	3	9	2	12
Total Dynamic Stability +30	0.7116	0.8986	0.6356	0.6259	6	7	7	8
DS+30/Cvp	0.6826	0.8779	0.5932	0.5937	8	12	8	11
Total Dynamic Stability +40	0	0	0	0.0000	15	16	15	16
DS+40/Cvp	0	0	0	0.0000	15	16	15	16
Wind A1/A2	0	0.9843	0	0.8352	15	1	15	1
$AREA_{0-15}$ not less than 0.07	0.5557	0.755	0.4776	0.4330	10	14	11	14
$AREA_{0-20}$ not less than 0.065	0.5532	0.7846	0.492	0.5259	11	13	10	13

Table 7-2 - Power fit R^2 values and ranking

7.1.7 Tables 7-1 and 7-2 above are exact copies (small) of Table 1 and 2 in the Tables Section 12 and are included here for reference.

7.1.8 Table 7-1 and Table 7-2 shows there are distinct trends to the data across the subsets. Generally, the exponential fit had the closer fit to the data. It can be seen that the traditional criteria measures did not show the closest fit with the three vessels tested. The wind heeling a/b criteria produced the best fit with an exponential R^2 value of 0.963. The area up to the GZmax and the total area under the GZ curve over the vertical prismatic coefficient were ranked at the top with all three vessels included. The area up to the GZmax has an R^2 value (exponential curve trend fit) of 0.919, while the area under the GZ curve was also highly ranked with an R^2 exponential fit of 0.914. Neither of these highly ranked measures are current IS code stability measure parameters. However, the Area 0-40 degrees was the 4^{th} highest ranked with the power curve fit, which is a current criteria measure.

7.1.9 The alternative criteria measures such as the Dynamic Stability (i.e. the total area under the GZ curve) and the variants of this criterion had a better fit with the three vessels than many of the standard criteria measures. The conventional vessel tested in this study provided the three widest ranging data points. The operating arrival load case for ST OLA was significantly more stable than the IS Limit case for that vessel. This is driven by the damage stability requirements for this vessel [25], which requires a lower KG to pass the damage criteria than the intact stability requirements. This therefore demonstrates the additional intact stability performance the vessel has by conforming to the damage stability criteria.

7.1.10 The first hypothesis was that the Critical Roll Index (capsize probability measure) was associated with the area up to the GZ max in line with the requirements for the criteria for Offshore Supply Vessels. With just the two high B/T vessels the alternative GZ criteria area 0-15 and 0-20 from the offshore supply vessel criteria did not show as good a fit as the area to GZmax term, which fitted well for all vessels, including the conventional vessel which had a GZmax close to 45 degrees. A similar pattern was shown with the both the exponential fit and the power fit curves.

7.1.11 The second hypothesis for alternative criteria for measuring stability performance was that the area under the GZ curve has a large influence on the probability of capsize of a ship. The method used to test this was to plot Critical Roll Index against the area under the GZ curve, the area from 30 degrees to RPS and from 40 degrees to RPS. The plots are provided in Annex C10, C11 and C12. The trend in these graphs showed that the total dynamic stability data aligns very closely with a exponential curve R^2 fit of 0.914 for all the vessels data, Figure C10. These could be alternative stability criteria with potentially a better relationship with the dynamic performance than some of the current intact stability criteria.

7.1.12 An extension to the second hypothesis was that the vertical prismatic coefficient (Cvp), which provides an indication of the slenderness of the underwater hull form, has a relationship with the dynamic stability performance. The area under the GZ curve was divided by the Cvp and plotted against the Critical Roll Index. The total area under the GZ curve over the Cvp provided no improvement over the total area under the GZ curve, with a power curve R^2 fit of 0.884, Figure C13.

7.1.13 To confirm the trends seen using the 45 degree critical roll angle and the distribution free trend line, a selection of calculations were made using the Gumbel data fit and a 70 degree critical angle. Figure C18 shows the total area under the GZ curve criteria plotted against the Critical Roll Index. The good trend fit seen in the original Figure C10 is still evident. The Critical Roll Index values are lower in Figure C18 due to the higher critical roll angle used.

7.1.14 Annex D contains the plots for the data for the high B/T vessels only. The criteria which improved significantly when the conventional vessel data was removed were the area 0-15 and 0-20 criteria, which originate from the offshore supply vessel criteria, which show a better correlation for the higher B/T vessels only. The GZmax value actually produced the highest ranked data fit with an exponential R^2 fit of 0.945. The wind heeling a/b criteria also remained highly ranked with the conventional vessel data removed.

7.2 Criteria Vs Critical Roll Index

7.2.1 Taking the Critical Roll Index for all the cases tested allowed the levels of the current criteria limits to be compared in a relative manner. By using the current criteria limit lines and the data trend lines from the Figures in Annex C, the current level of risk of reaching the critical roll angle (45 degrees) could be evaluated at each of the current intact stability criteria limit levels. Table 7-3 below lists all of the current levels.

Criteria Parameter	Current IS Limit	Critical roll Risk level in a Seaway
GM	0.15m	Not reached
Area 0-30	0.055 mrads	$8x10^{-2}$
Area 0-40	0.09 mrads	$8x10^{-2}$
Area 30-40	0.03 mrads	$4x10^{-2}$
GZ max	Not less than 0.2	$2x10^{-2}$
Angle of GZmax	Not less than 25 degs	$8x10^{-2}$
a/b	1.0	$7x10^{-3}$

Table 7-3 - Capsize Risk for Current Criteria Limit (exponential trend line)

7.2.2 Table 7-3 shows that many of the current IS code criteria limits are reached at similar values of critical roll risk, at around the $8X10^{-2}$ level. The major exception to this is the a/b wind criteria, where there criteria level is reached at 7×10^{-3}. This was using approximated data with a fixed 25 degree count back angle which could account for this. This measure does, however, still produce the best fit of 0.963 and is the best current measure.

7.2.3 Table 7-4 below contains the other best ranking potential criteria measures that were examined and the level required to provide an index of 2×10^{-2} equal to the lowest current IS limit (excluding a/b due to the fixed 25 degree angle used) including the MV ST OLA data. To equate the Critical Roll Index to the current actual arrival operating level for this vessel (lowest GM currently operated at due to the damage criteria limits) then lower values are required.

Criteria Parameter	Equivalent Level for a Critical Roll Index level of $2x10^{-2}$
Dynamic Stability	0.24 mrads
Dynamic Stability / Cvp	0.34
Area to GZmax	0.14 mrads
Area 0-20 (high B/T)	0.06 mrads
Area 0-15 (high B/T)	0.04 mrads

Table 7-4 - Capsize Risk for Alternative Criteria Limits (Exponential trend line)

7.2.4 The Area 0-15 criteria can be seen in Table 7-4 to provide an equivalent critical roll index at 0.04 and so the current proposed 0.07 m.rads is greater. However, the vessels tested do not have a GZ curve that peaks that low. The Area 0-20 criteria requires an area of 0.065 m.rads in the proposed IS code. To obtain an equivalent Critical Roll index an area of 0.06 is required based on the high B/T vessel data, which is just below this value, where their GZmax values are above 20 degrees (23 to 25 degrees). Considering the area to the GZ max for the two larger B/T vessels at the three conditions, it can be seen that they will currently pass the proposed IS code area criteria, which is dependant on the actual GZmax angle when it is between 20 and 30 degrees. To achieve an equivalent Critical Roll Index then an area to GZmax of 0.14 is required for these vessels with the angle of GZmax between 20 and 25 degrees. The area to GZmax ranked highly for all vessels and the high B/T vessels when considered on their own. This suggests that this criterion provides a good indication of the dynamic stability performance.

8 Conclusions

8.1 Model Experiment Comparison

8.1.1 Roll motion of the 1/30th scale model of MV St OLA was compared with the FREDYN simulations. In the operating condition close agreement was found and results were within 10% in most cases. This included the standard roll RAO, extreme roll in steep regular waves and RMS roll motion in irregular seas.

8.1.2 The results for the IS limit case showed greater damping in FREDYN compared to the experiment at the peak in the RAO curves. The extreme roll cases showed around 20% under prediction in the simulations at the higher wave periods. At the shorter wave period the result was within 2%. This suggests that there is a possible roll damping scaling effect at the slow roll cases at this lower GM condition, which does not occur as the waves get shorter and the roll rate increases. It was shown that FREDYN was able to adequately model this type of vessel in moderate to extreme wave conditions.

8.2 Dynamic Stability Vs Static Stability Criteria

8.2.1 The current GZ area criteria did not produce the best data fit, compared to some alternative stability measures, with the exponential trend line and power curve trend lines using all of the vessels in the data set.

8.2.2 For the vessels tested, the simplified a/b wind criteria (using a fixed 25 degree count back angle), area under the GZ curve, area under the GZ curve over the vertical prismatic coefficient (Cvp) and the area up to GZmax were shown to be the best fitting criteria with the complete data set for the three test vessels.

8.3 Equivalent Levels of Critical Roll Index

8.3.1 By reviewing where the limit lines cross the trend lines for the data, it has been shown that nearly all of the existing current intact stability criteria limits are reached at similar values of Critical Roll Index, at 8×10^{-2}. The large exception to this is the simplified weather criteria a/b (using a fixed 25 degree count back angle), where there criteria level is reached at 7×10^{-3}.

8.3.2 The Area 0-30 criteria current limit was easily surpassed in all but one condition tested for the conventional vessel (ST OLA). The proposed Area 0-15 and Area 0-20 criteria for vessels with early peaking GZ curves did not provide a good data fit for the high B/T vessels tested. However the area to GZmax was a highly ranked criteria, which fitted all the vessels and the high B/T vessels tested had GZ curves that peaked between 20 and 30 degrees. To achieve the equivalent Critical Roll Index as the IS Limit case, an area of 0.035 mrads would be required, so the current 0.07 m.rads would be sufficient. This should be used with caution, as the vessels tested did not have GZ curves that peaked between 15 and 20 degrees. The Area 0-20 criteria (closer to the vessels tested but still lower) requires an area of 0.065 m.rads. To obtain the equivalent Critical Roll Index, an area of 0.060 m.rads would be required for the vessels tested. It should be noted that the GZ curves peak at over 20 degrees (at between 23 and 25 degrees) for the vessels tested.

8.3.3 Considering the area to the GZmax for the two larger B/T vessels at the three conditions tested, they currently pass the new proposed IS code area criteria which is scaled, based on actual GZmax angle, when it is between 20 and 30 degrees.

8.3.4 The area to the GZmax criteria was shown to produce one of the best data fits of all the criteria tested for the complete set of data, not just the two high B/T vessels. This suggests that this criteria measure would be a good indication of stability performance. To achieve a critical roll index equivalent of the IS limited case, an area to GZmax value of 0.14 is required. This may be particularly suitable for vessels with GZ curves peaking below 30 degrees.

8.4 Alternative Static Stability Criteria

8.4.1 There are currently no stability criteria for the total area under the GZ curve (dynamic stability) or the area under the GZ over vertical prismatic coefficient in the current IS code. The trend lines on the complete data set give a data fit of 0.914, which is better than most of the standard criteria measures tested. To achieve an equivalent level of critical roll index to the IS code limiting case for the conventional vessel, then a total area under the GZ curve of greater than 0.2 m.rads is required or a GZ area / Cvp of 0.34.

9 Recommendations

9.1 Recommendations for Criteria for larger B/T Vessels

9.1.1 It is recommended that for vessels like those tested in this study that have a low peaking GZ curve but pass the other IS Code requirements, additional measures should be made. The area to GZmax and the total area under the GZ curve should be evaluated to confirm that the values are at least as great as those derived in this project in addition to meeting the other IS code requirements.

9.2 Recommendations for future studies

9.2.1 It is recommended that further calculations are performed with other small domestic vessels in the UK fleet to investigate further and expand the data set with new and older hull forms to confirm the findings and Critical Roll Index levels associated with the current intact stability criteria. Vessels with very low peaking GZ curves between 15 and 20 degrees are particularly recommended.

9.2.2 It is recommended that for novel vessel designs the alternative criteria measures are used to provide confidence in the level of safety provided by the vessel. Further FREDYN studies on novel vessels will provide further confidence in the alternative criteria terms.

10 References / Bibliography

[1] IMO Intact Stability Code, Res. A.562.

[2] Umeda, N., Matsuda, A., Hamamoto, M. and Suzuki, S. *Stability Assessment for Intact Ships in the Light of Model Experiments*. Journal of Marine Science and Technology, 4:2: 45-57. 1999.

[3] Francescutto, A and Serra, A. *Weather Criterion for Intact Stability of Large Passenger Vessels*. Proceedings of the 5th International Workshop on Stability and Operational Safety of Ships. University of Trieste, Italy, 12-13 September 2001.

[4] Eliopoulou, E. and Papanikolaou, A. *Review of Design Features and Stability Characteristics of Pre- and Post- SOLAS 90 RORO Passenger Ships*. Proceedings of the 5th International Workshop on Stability and Operational Safety of Ships. University of Trieste, Italy, 12-13 September 2001.

[5] Francescutto, A and Serra, A. *Experimental Tests on Ships with Large Values of B/T, OG/T and Roll Period*. 6th International Ship Stability Workshop Proceedings. New York, October 13-16 2002.

[6] Cramer, H. and Tellkamp, J. *Towards the Direct Assessment of a Ship's Intact Stability*. 6th International Ship Stability Workshop Proceedings. New York, October 13-16 2002.

[7] Blume, P. *Development of new stability criteria for modern dry cargo vessels*. Proceedings of PRADS – Practical Design of Ships and Marine Units. Elsevier, Troneheim. 1987.

[8] IMO-SLF. *Review of the Intact Stability Code*. IMO-SLF 45/6/3, London, 2002.

[9] IMO-SLF. *Calculations using the proposed factors s and r for the weather criterion.* IMO-SLF 46/6/7, London, 2003.

[10] IMO-SLF. *Severe wind and rolling criterion (weather criterion)*. IMO-SLF 46/6/10, London, 2003.

[11] IMO-SLF. *Proposal on draft explanatory notes to the severe wind and rolling criterion*. IMO-SLF 48/4/5, London, 2005.

[12] Francescutto, A. *Intact Ship Stability – The Way Ahead*. 6th International Ship Stability Workshop Proceedings. New York, October 13-16 2002.

[13] Turan, O. and Tuzcu, C. *Towards the Performance Based Approach for Stability of Cruise Vessels*. Proceedings of 8th International Conference on the Stability of Ships and Ocean Vehicles. Spain, 2003.

[14] Yoon, HK. Kim, SY. Hong, SY. Kim, YS. Kim, JH. and Lee, SJ. *Application and Review on Interim Guidelines for Alternative Assessment of the Weather Criterion.* Proceedings of 9th International Conference on Stability of Ships and Ocean Vehicles. Rio de Janeiro, 25-29 September 2006.

[15] Taguchi, H. Ishida, S. and Sawada, H. *A Trial Experiment on the IMO Draft Guidelines for Alternative Assessment of the Weather Criterion*. Proceedings of the 8th International Ship Stability Workshop. Istanbul, Turkey. 6-7 October 2005.

[16] Ishida, S. Taguchi, H. and Sawada, H. *Evaluation of the Weather Criterion by Experiments and its Effect to the Design of a RoPax Ferry*. Proceedings of 9th International Conference on Stability of Ships and Ocean Vehicles. Rio de Janeiro, 25-29 September 2006.

[17] Vassalos, D. Jasionowski, A. and Cichowicz, J. *Weather Criterion – Questions and Answers*. Proceedings of 8th International Conference on the Stability of Ships and Ocean Vehicles. Spain, 2003.

[18] Matusiak, J. and Hamberg, K. *Considerations on the Weather Criterion Applicability for the Stability Assessment of Large Vessels*. Proceedings of 9th International Conference on Stability of Ships and Ocean Vehicles STAB2006. Rio de Janeiro, 25-29 September 2006.

[19] Cramer, H. Kruger, S. and Mains, C. *Assessment of Intact Stability – Revision and Development of Stability Standards, Criteria and Approaches*. Proceedings of 7th International Ship Stability Workshop. Shanghai, China. November 1-3 2004.

[20] Krueger, S. and Kluwe, F. *Development of Dynamic Stability Criteria from Direct Seakeeping Simulations*. Proceedings of 9th International Marine Design Conference. Ann Arbor, Michigan. 16-19 May, 2006.

[21] IMO-SLF. *Proposal of a probabilistic intact stability criterion*. Agenda item 5, submitted by Germany. IMO-SLF 49/5/2. April 2006.

[22] IMO-SLF. *Restructured IS Code*. IMO-SLF 49 Annex. April 2006.

[23] Hughes, T. Naval Stability Standards Working Group: Intact Stability Work Plan.

[24] Sarchin, TH and Goldberg, LL. *Stability and Buoyancy Criteria for US Naval Surface Ships*. SNAME Transactions. v70, 1962.

[25] Three Quays Marine Services. *St. Ola Trim and Stability Book*. Report No. 94-082. Prepared for P&O Scottish Ferries (Aberdeen) Ltd. April 1995.

[26] *Linesplan drawings* MCM (Marine Design).

[27] *General Arrangement*. MCM (Marine Design). 8th Jan 1992. Drawing No. MCM 1447

[28] *Details of Installation of Stabilisers*. MCM (Marine Design). 8th Jan 1992. Drawing No. MCM 1468

[29] *Tank Plan*. MCM (Marine Design). 28th Feb 1992. Drawing No. MCM 1529

[30] *Außenhaut (Shell Expansion)*. Jos. L. Meyer Papenburg (Ems). 28th April 1970. Drawing No. 564/04

[31] *After Body line drawing*. Jos. L. Meyer Papenburg (Ems). Drawing No. 564/09

[32] McTaggart, KA. *Improved Modelling of Capsize Risk in Random Seas*. Defence Research Establishment Atlantic. July 2000

[33] Lloyd, ARJM. *Seakeeping: Ship Behaviour in Rough Weather.* Revised Edition. Published by the author. Available from Royal Institution of Naval Architects, 10 Upper Belgrave Street, London. 1998.

[34] Peters AJ “A Comparison of Ship Capsize Risk with Static Stability Criteria – Working Paper” - QINETIQ/D&T/SEA/WP0702785/1.0 , March 2007

[35] Sea Technology Group, “Stability of Surface Ships, Part One: Conventional Ships”, Sea Systems Publication No 24, Defence Procurement Agency, 1999.

[36] Bales S.L, Lee, WT and Voelker J.M (1981) Standardised Wave and Wind Environments for NATO Operational Areas.
[37] McTaggert K.A, DeKat J.O 'Capsize Risk of Intact Frigates in Irregualr Seas', SNAME Transactions 2000.

11 Glossary

IMO	International Maritime Organisation
SLF	The Stability, Load-line and Fishing vessel (SLF) subcommittee of IMO
IS Code	Intact Stability Code
RAO	Response Amplitude Operator
RMS	Root Mean Squared
Critical Roll Index	The relative probability of exceeding a defined critical roll angle in 1hr for all considered sea states. It is used as a relative "capsize" probability depending on the capsize definition used.

12 Tables

Exponential		Value				Rank		
Parameter	All Data	LOTI & Hebrides	All Data	LOTI & Hebrides	All Data	LOTI & Hebrides	All Data	LOTI & Hebrides
	All Waves	All Waves	Upto Mid SS7	Upto Mid SS7	All Waves	All Waves	Upto Mid SS7	Upto Mid SS7
GM_F(m) not less than 0.15	0.3423	0.5129	0.2380	0.1969	17	16	17	15
$AREA_{0-30}$ not less than 0.055	0.5714	0.8717	0.4983	0.5783	10	7	11	6
$AREA_{0-40}$ not less than 0.09	0.7186	0.8825	0.6270	0.5951	8	5	8	5
$AREA_{30-40}$ not less than 0.03	0.8060	0.8956	0.6090	0.6171	5	3	9	3
Area to GZ max	0.9195	0.8375	0.8160	0.5367	2	8	3	9
Angle of GZ_{max} not less than 30	0.3790	0.8864	0.3769	0.6717	16	4	14	4
GZ_{max} not less than 0.2	0.7843	0.9456	0.7438	0.7420	6	1	5	2
Total Dynamic Stability	0.9143	0.8081	0.8222	0.5036	3	9	2	10
RPS	0.3825	0.8770	0.3461	0.6134	15	6	16	7
DS/Cvp	0.8840	0.7530	0.7596	0.4308	4	11	4	12
Total Dynamic Stability +30	0.7237	0.7367	0.6622	0.4315	7	12	6	8
DS+30/Cvp	0.6989	0.7037	0.6370	0.3902	9	13	7	11
Total Dynamic Stability +40	0.5414	0.5190	0.5110	0.2353	11	15	10	16
DS+40/Cvp	0.5241	0.4381	0.4939	0.1616	12	17	12	16
Wind A1/A2	0.9634	0.9386	0.9290	0.8352	1	2	1	1
$AREA_{0-15}$ not less than 0.07	0.4659	0.6893	0.3692	0.4330	14	14	15	14
$AREA_{0-20}$ not less than 0.065	0.4891	0.7846	0.4022	0.5292	13	10	13	13

Table 1 : Criteria Ranking based on Exponential Curve R^2 curve fit

POWER								
	Value				Rank			
Parameter	All Data	LOTI & Hebrides	All Data	LOTI & Hebrides	All Data	LOTI & Hebrides	All Data	LOTI & Hebrides
	All Waves	All Waves	Upto Mid SS7	Upto Mid SS7	All Waves	All Waves	Upto Mid SS7	Upto Mid SS7
GM_F(m) not less than 0.15	0.4815	0.6007	0.3843	0.2810	12	15	12	15
$AREA_{0-30}$ not less than 0.055	0.6051	0.9119	0.5521	0.6392	9	5	9	6
$AREA_{0-40}$ not less than 0.09	0.7232	0.9295	0.6606	0.6716	4	4	6	5
$AREA_{30-40}$ not less than 0.03	0.6878	0.9415	0.7058	0.7336	7	3	4	3
Area to GZ max	0.9255	0.9032	0.8605	0.6232	1	6	1	9
Angle of GZ_{max} not less than 30	0.3565	0.8980	0.3504	0.6856	14	8	13	4
GZ_{max} not less than 0.2	0.7174	0.9771	0.6884	0.7853	5	2	5	2
Total Dynamic Stability	0.8617	0.8891	0.7831	0.6050	2	11	3	10
RPS	0.4085	0.8908	0.3174	0.6347	13	10	14	7
DS/Cvp	0.8507	0.8954	0.7834	0.5401	3	9	2	12
Total Dynamic Stability +30	0.7116	0.8986	0.6356	0.6259	6	7	7	8
DS+30/Cvp	0.6826	0.8779	0.5932	0.5937	8	12	8	11
Total Dynamic Stability +40	0.0000	0.0000	0.0000	0.0000	15	16	15	16
DS+40/Cvp	0.0000	0.0000	0.0000	0.0000	15	16	15	16
Wind A1/A2	0.0000	0.9843	0.0000	0.8352	15	1	15	1
$AREA_{0-15}$ not less than 0.07	0.5557	0.7550	0.4776	0.4330	10	14	11	14
$AREA_{0-20}$ not less than 0.065	0.5532	0.7846	0.4920	0.5259	11	13	10	13

Table 2 : Criteria Ranking based on Power Curve R^2 curve fit

A Ship Details

A.1 Solid Model Images

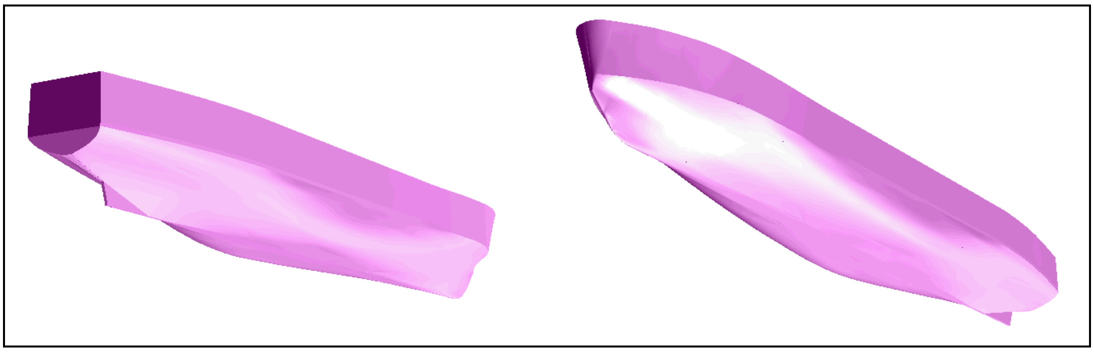

Figure A1 MV ST. OLA Solid Model

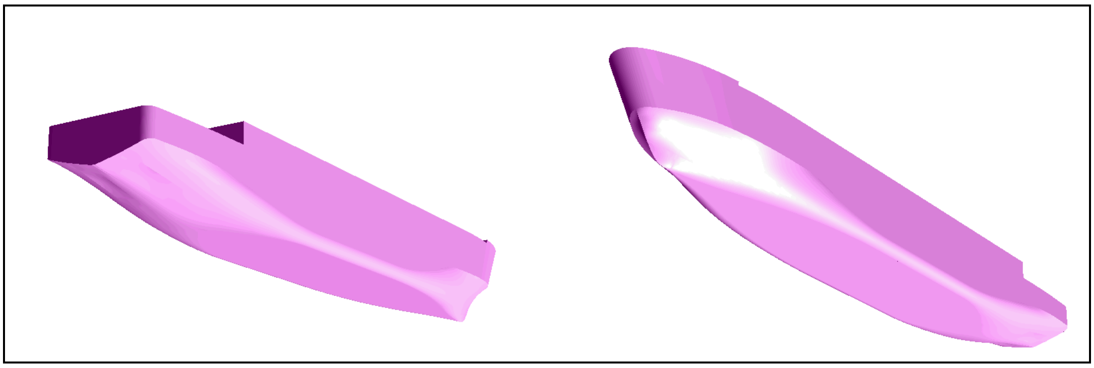

Figure A2 MV HEBRIDES Solid Model

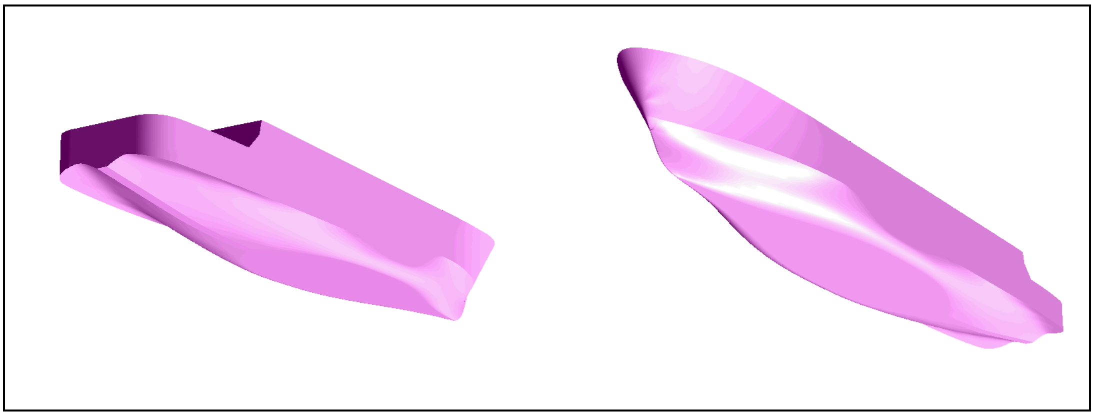

Figure A3 MV LORD OF THE ISLES Solid Model

B Model Photographs

Figure B1 – Model EAN – 1/30th scale model of MV ST OLA

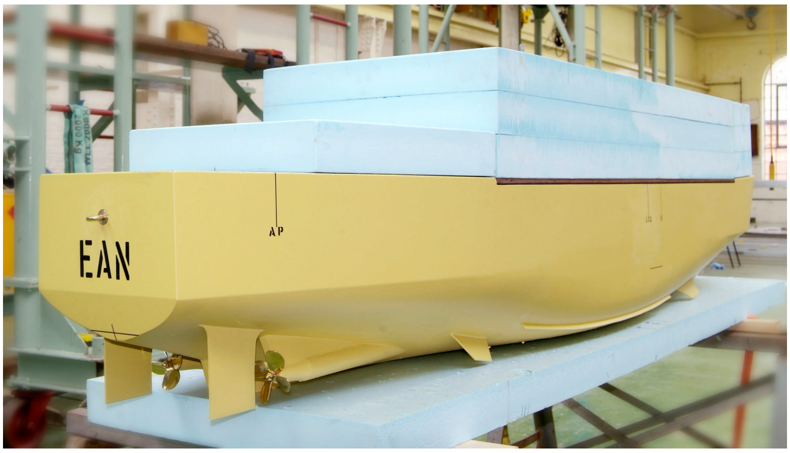

Figure B2 – Model EAN – 1/30th scale model of MV ST OLA

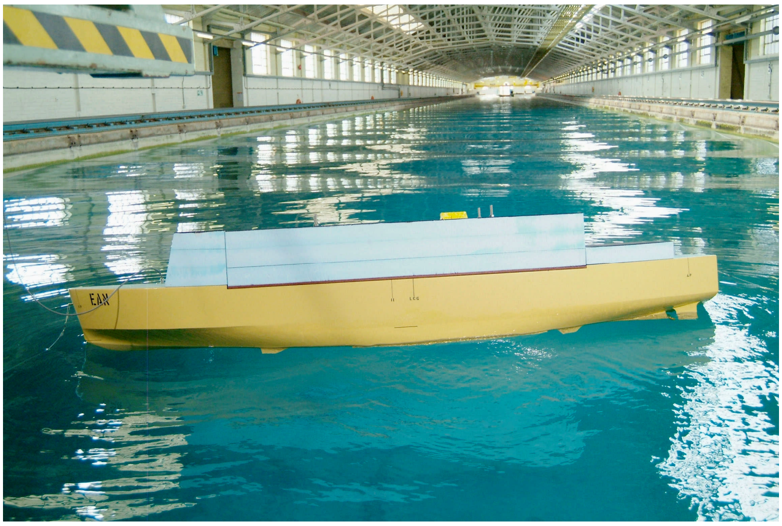

Figure B3 – Model EAN – EAN in QinetiQ Ship Tank

C Critical Roll Index Results – All Data

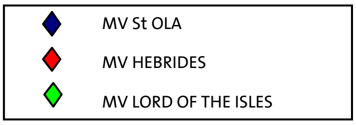

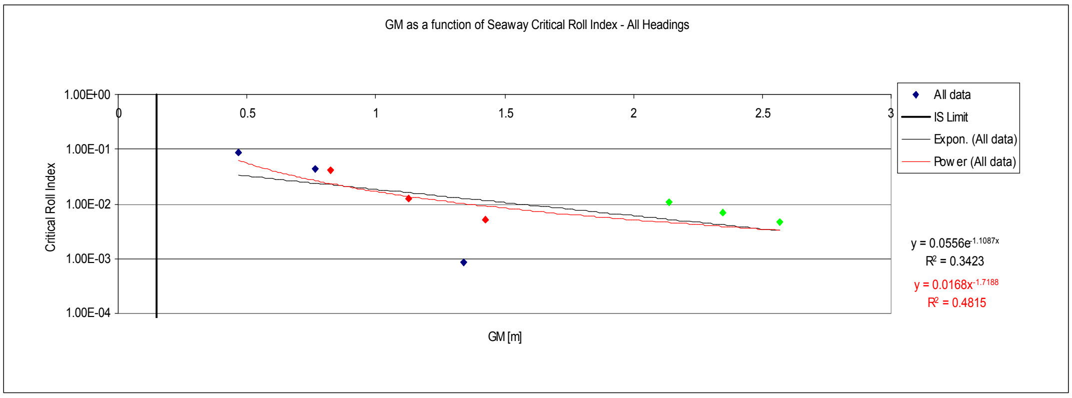

Figure C1 – GM as a function of seaway Critical Roll Index

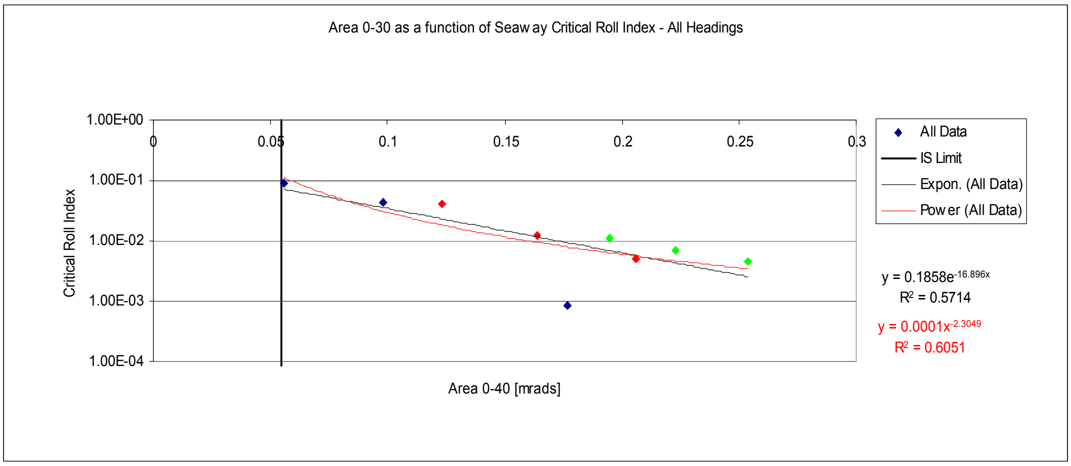

Figure C2 – Area 0-30 as a function of seaway Critical Roll Index

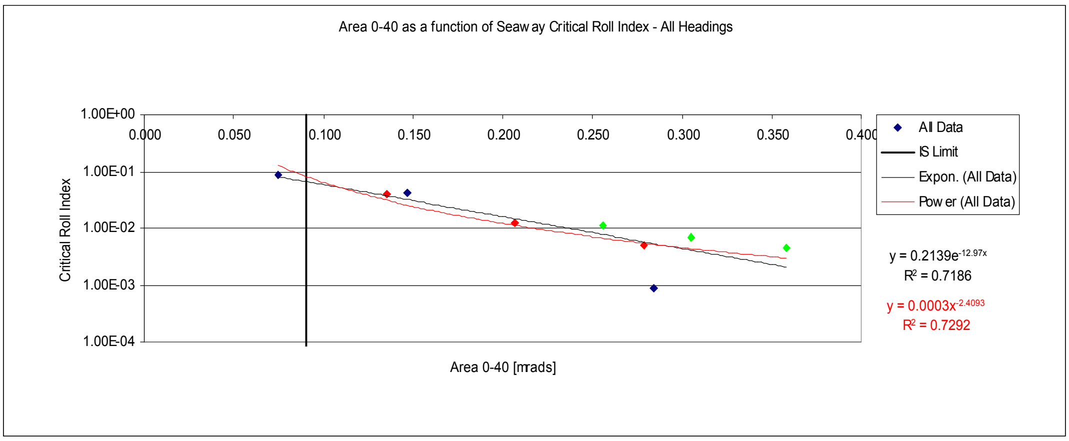

Figure C3 – Area 0-40 as a function of seaway Critical Roll Index

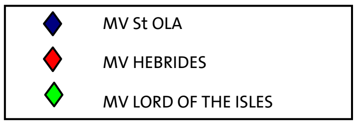

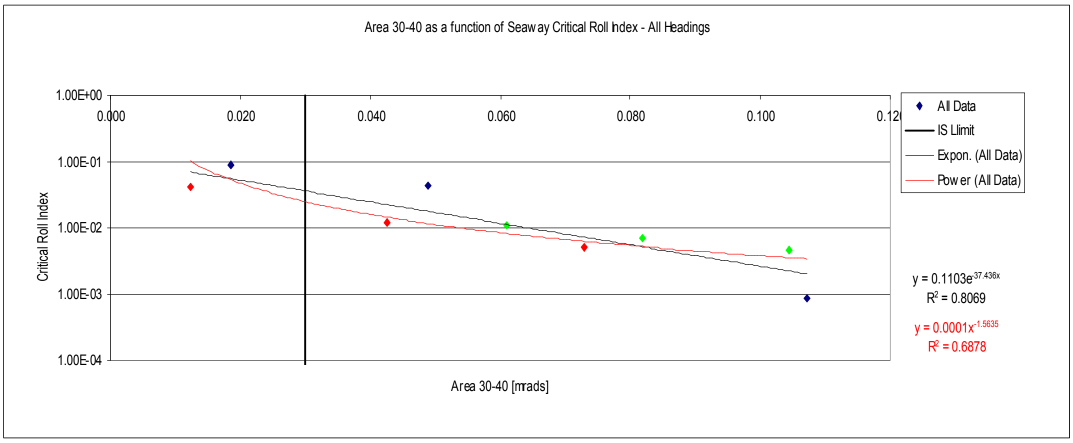

Figure C4 – Area 30-40 as a function of seaway Critical Roll Index

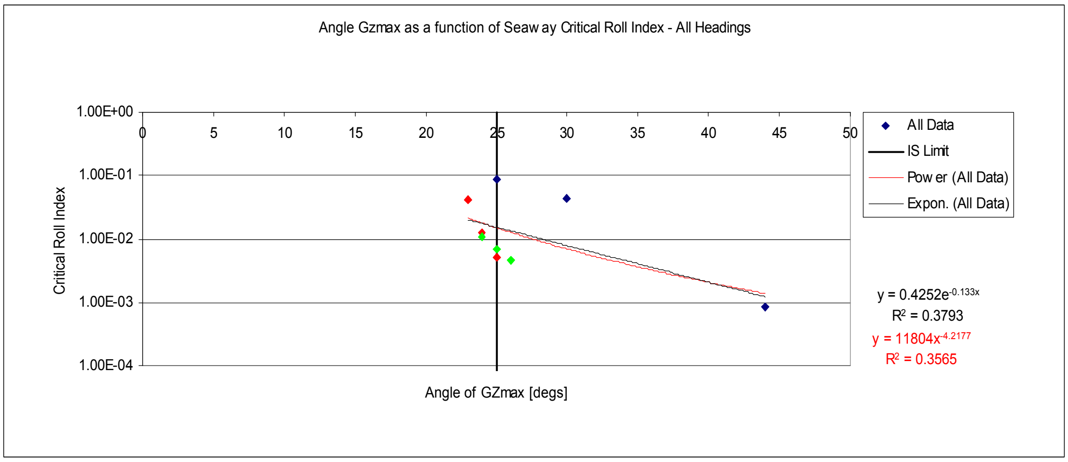

Figure C5 – Angle GZmax as a function of seaway Critical Roll Index

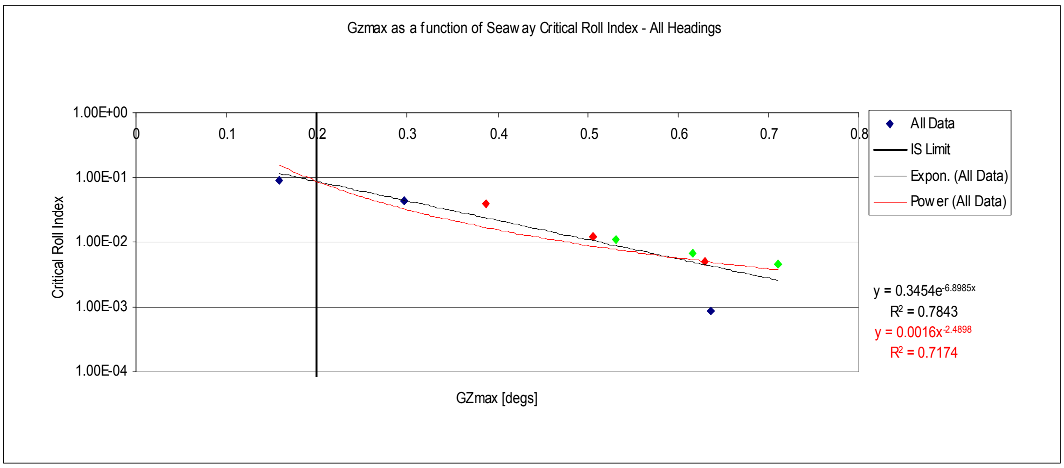

Figure C6 – GZmax as a function of seaway Critical Roll Index

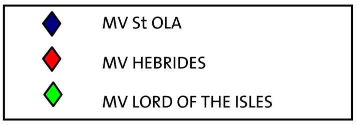

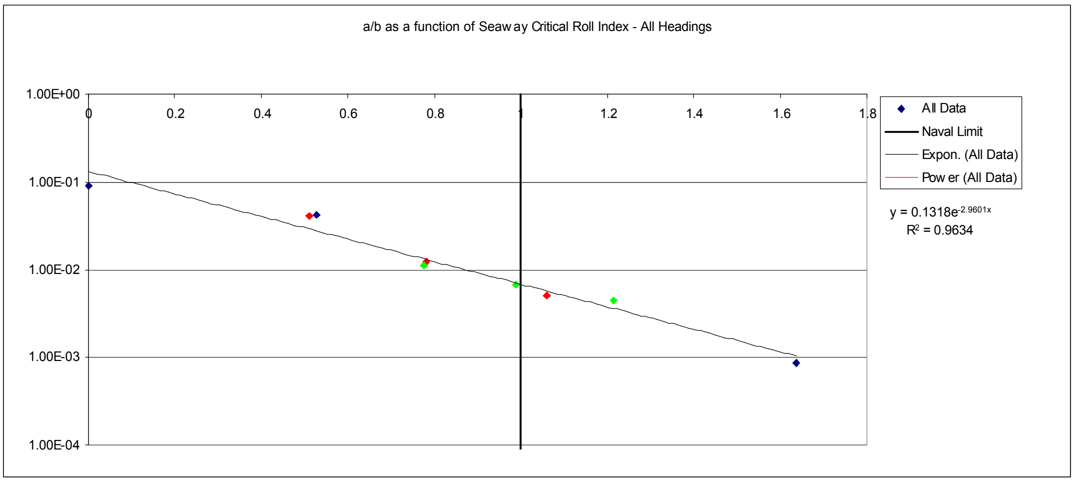

Figure C7 – a/b as a function of seaway Critical Roll Index

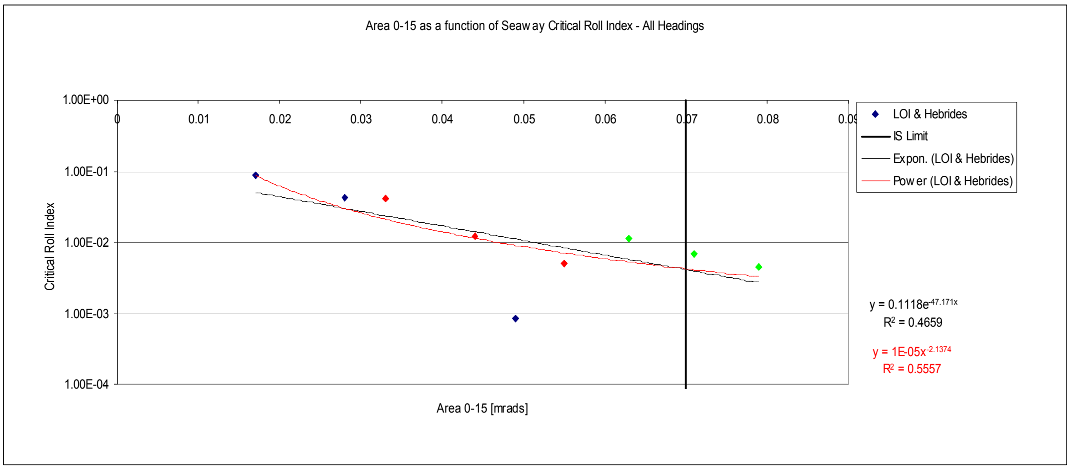

Figure C8 – Area 0-15 as a function of seaway Critical Roll Index

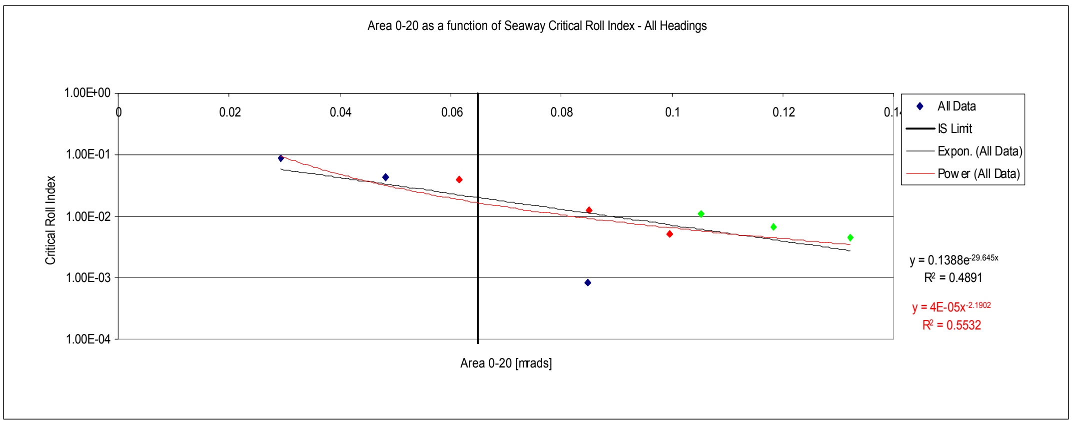

Figure C9 – Area 0-20 as a function of seaway Critical Roll Index

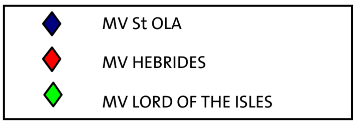

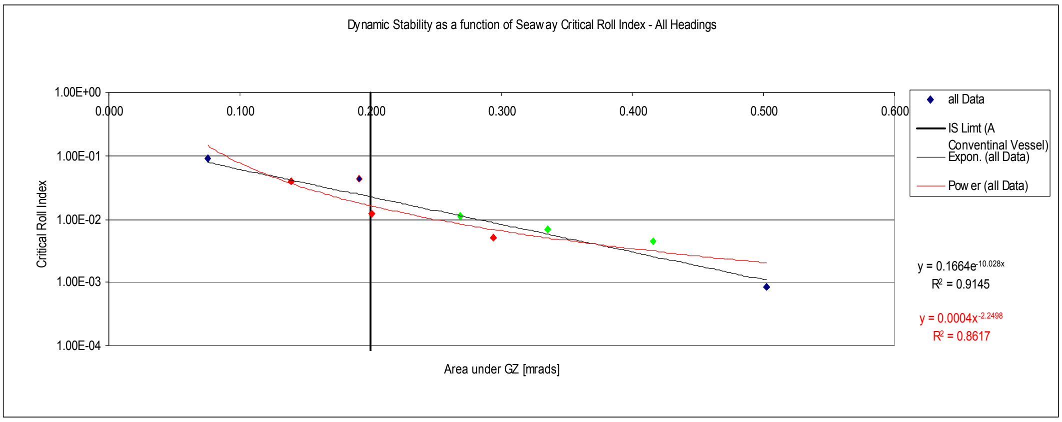

Figure C10 – Area under the GZ curve as a function of seaway Critical Roll Index

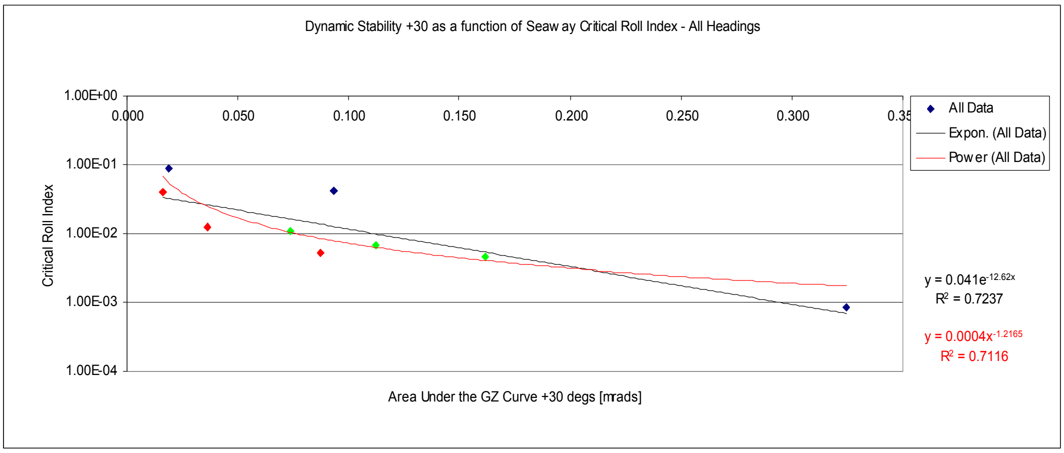

Figure C11 – Area under the GZ curve+30degs as a function of seaway Critical Roll Index

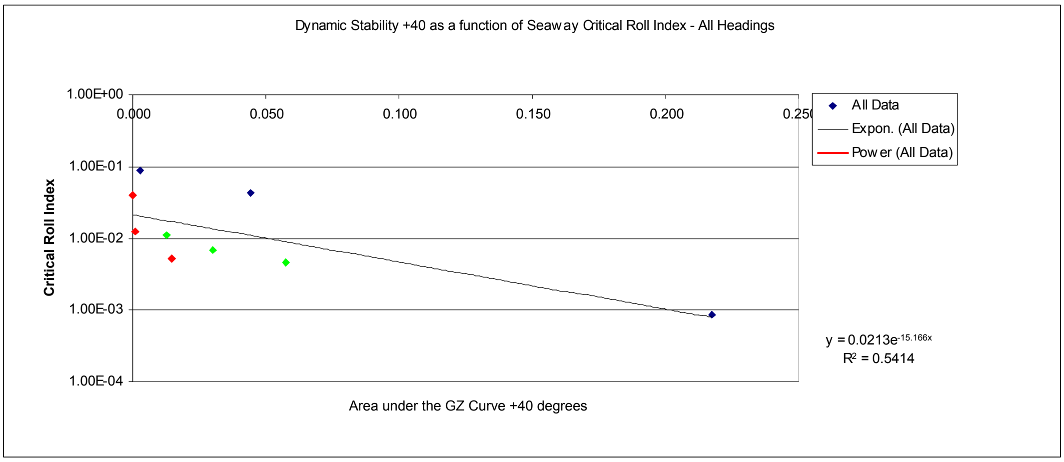

Figure C12 – Area under the GZ curve +40degs as a function of seaway Critical Roll Index

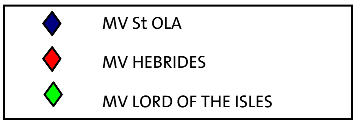

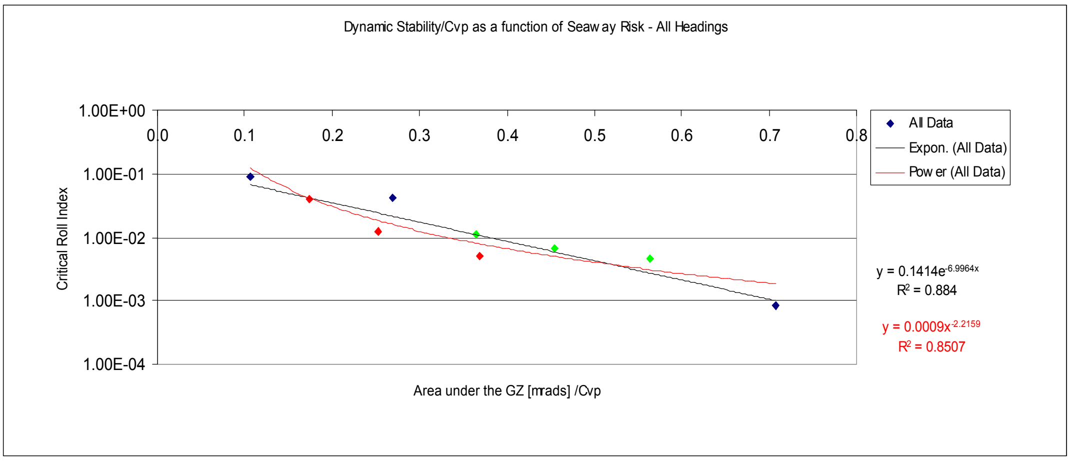

Figure C13 – Area under the GZ curve/Cvp as a function of seaway Critical Roll Index

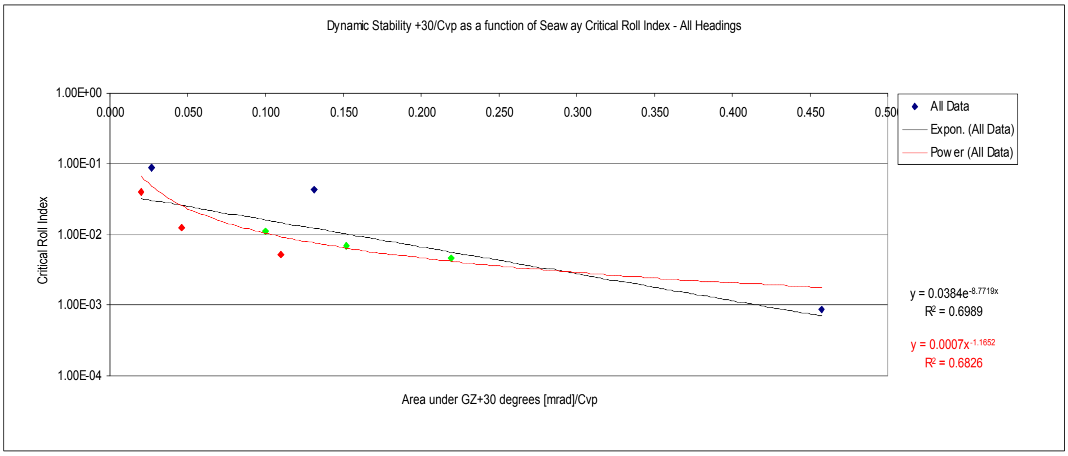

Figure C14 – Area under the GZ curve +30degs/Cvp as a function of seaway Critical Roll Index

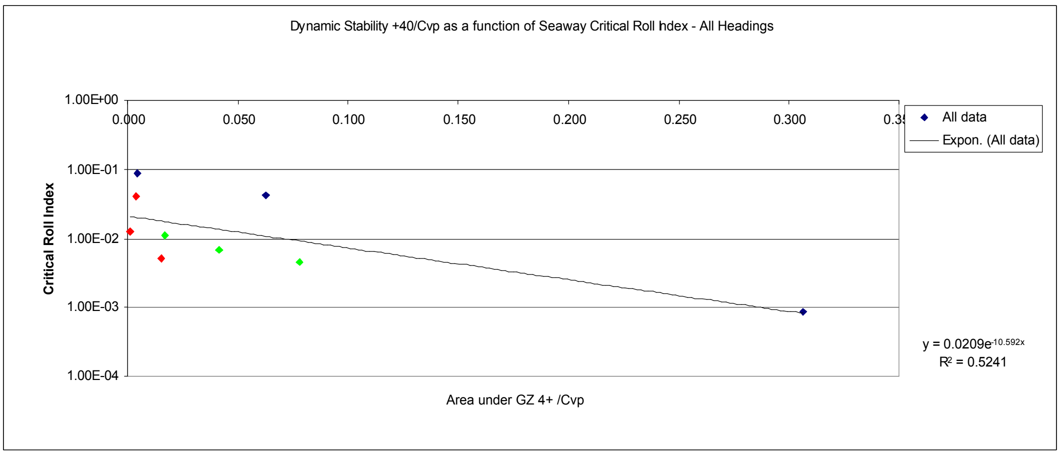

Figure C15 – Area under the GZ curve +40degs/Cvp as a function of seaway Critical Roll Index

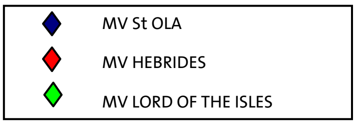

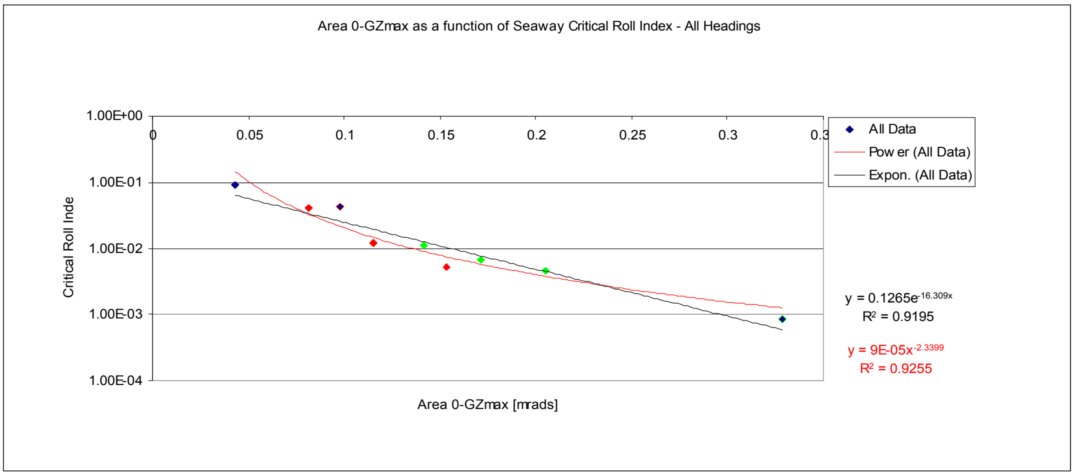

Figure C16 – Area under the GZ curve to GZmax as a function of seaway Critical Roll Index

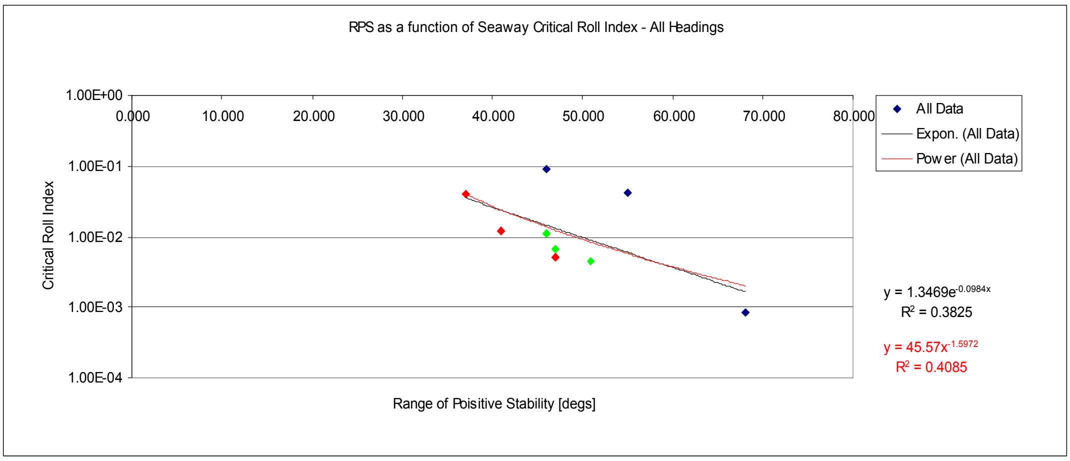

Figure C17 – Range of Positive Stability as a function of seaway Critical Roll Index

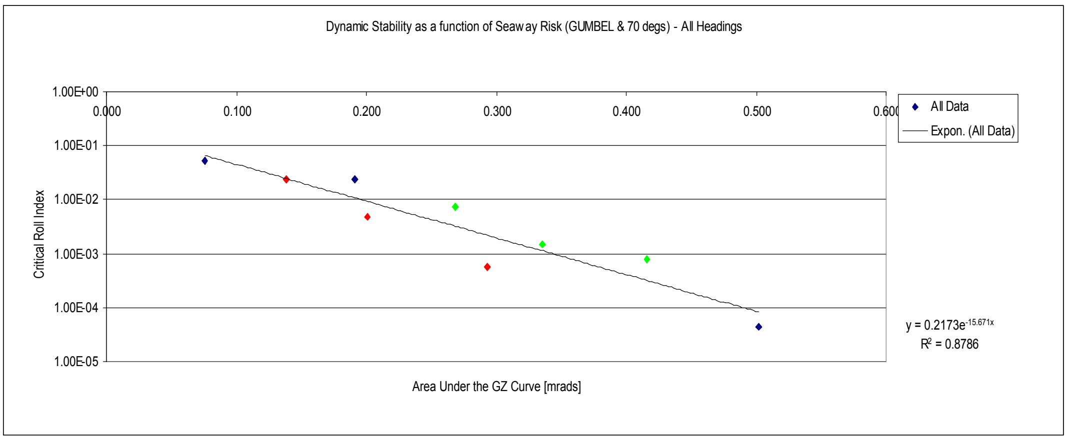

Figure C18 – Area under the GZ as a function of seaway Critical Roll Index (using Gumbel fit and 70 degree critical roll angle)

D Critical Roll Index Results – High B/T Vessels

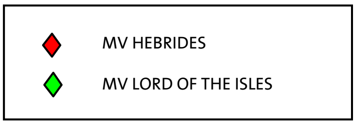

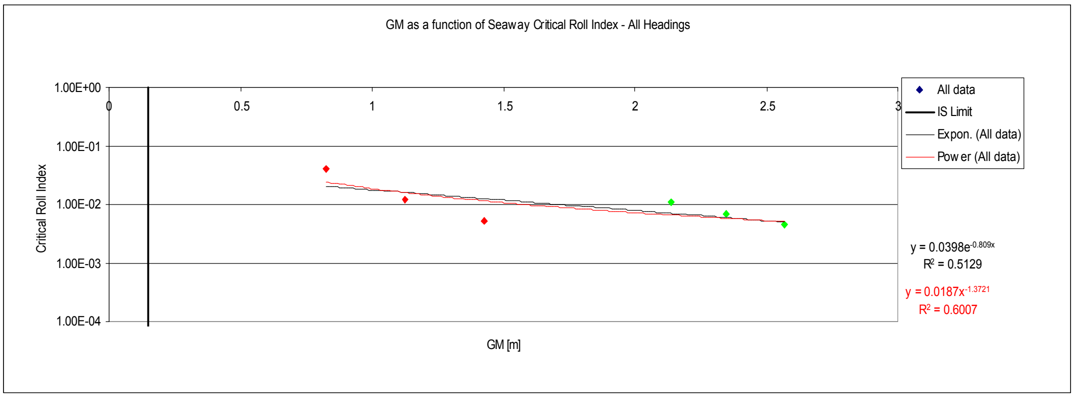

Figure D1 – GM as a function of seaway Critical Roll Index

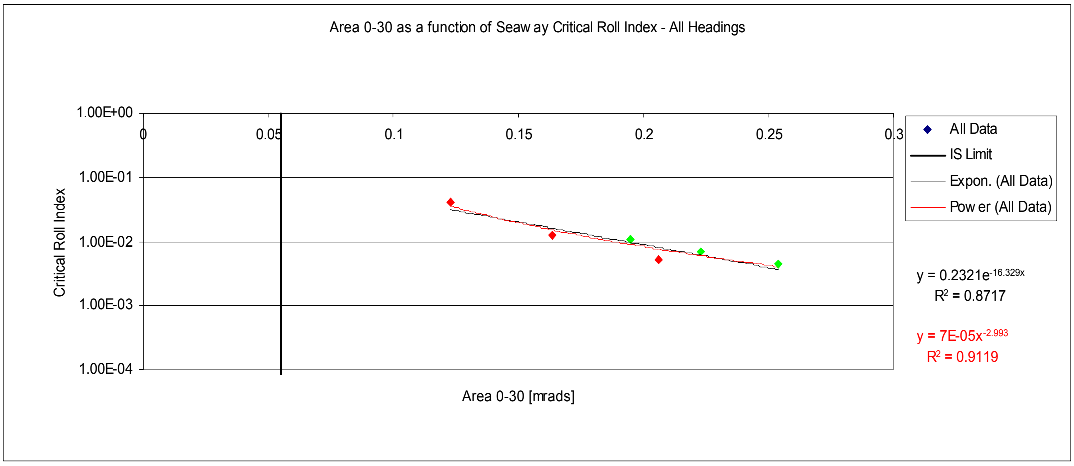

Figure D2 – Area 0-30 as a function of seaway Critical Roll Index

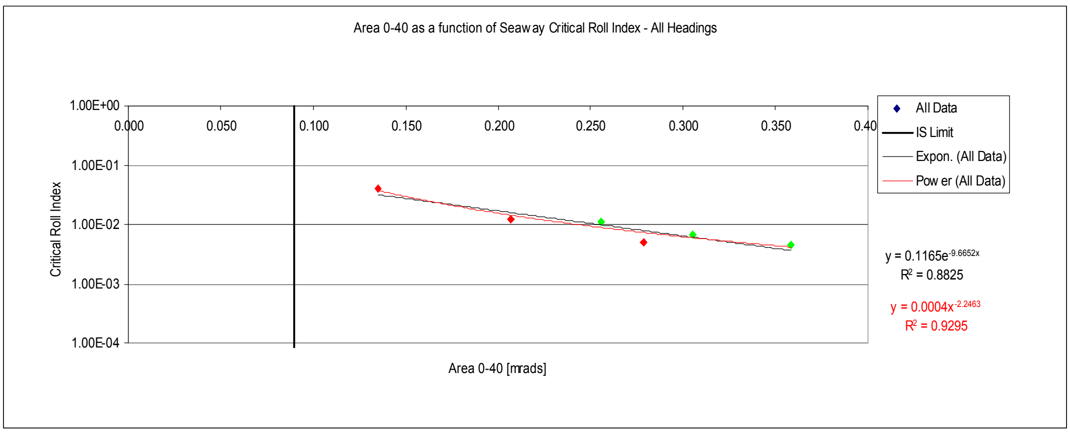

Figure D3 – Area 0-40 as a function of seaway Critical Roll Index

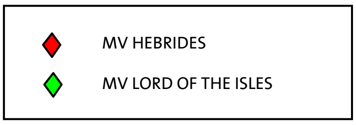

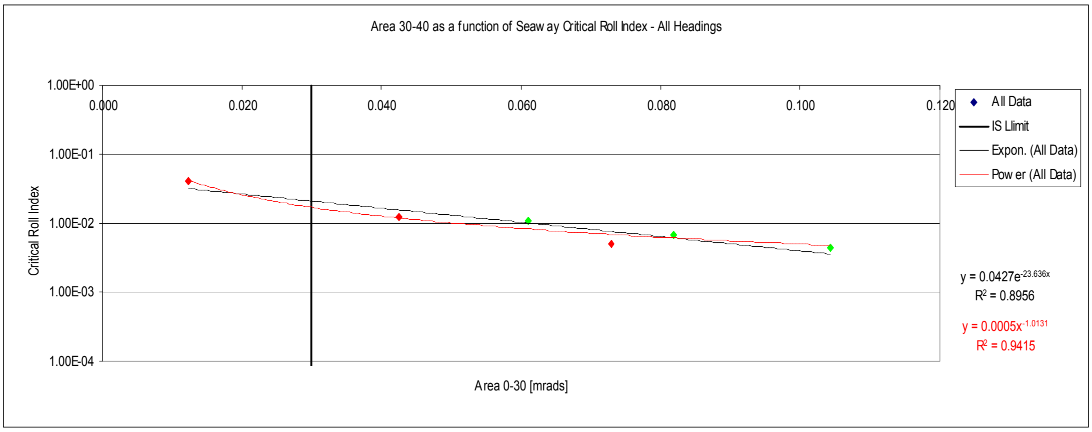

Figure D4 – Area 30-40 as a function of seaway Critical Roll Index

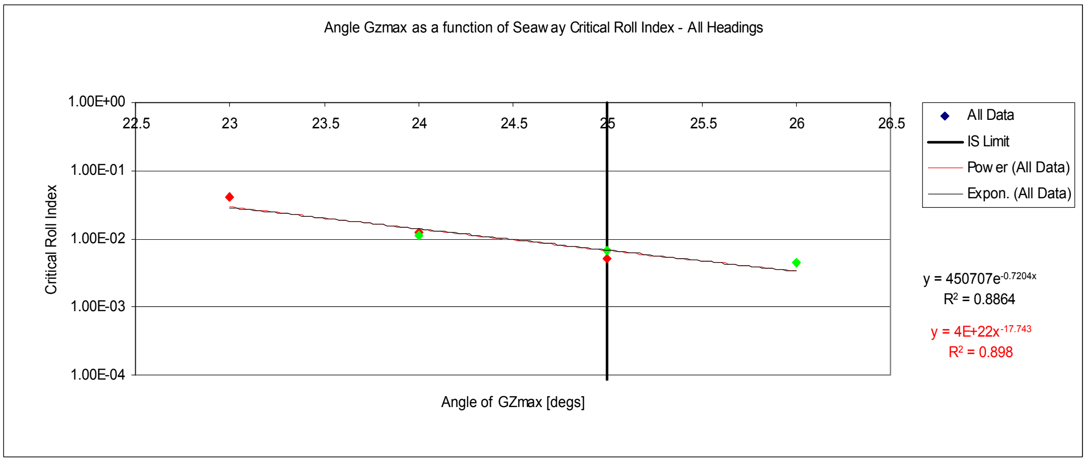

Figure D5 – Angle GZmax as a function of seaway Critical Roll Index

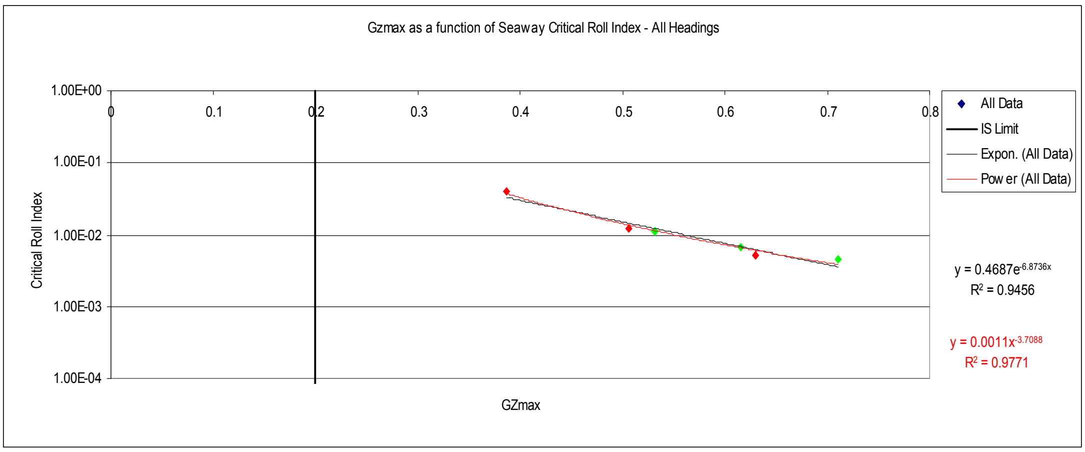

Figure D6 – GZmax as a function of seaway Critical Roll Index

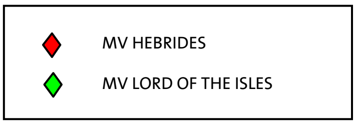

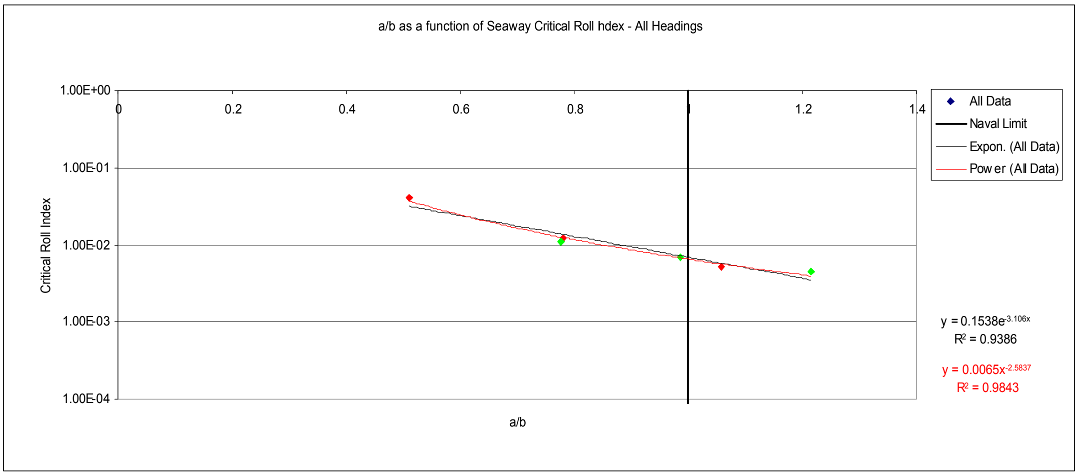

Figure D7 – a/b as a function of seaway Critical Roll Index

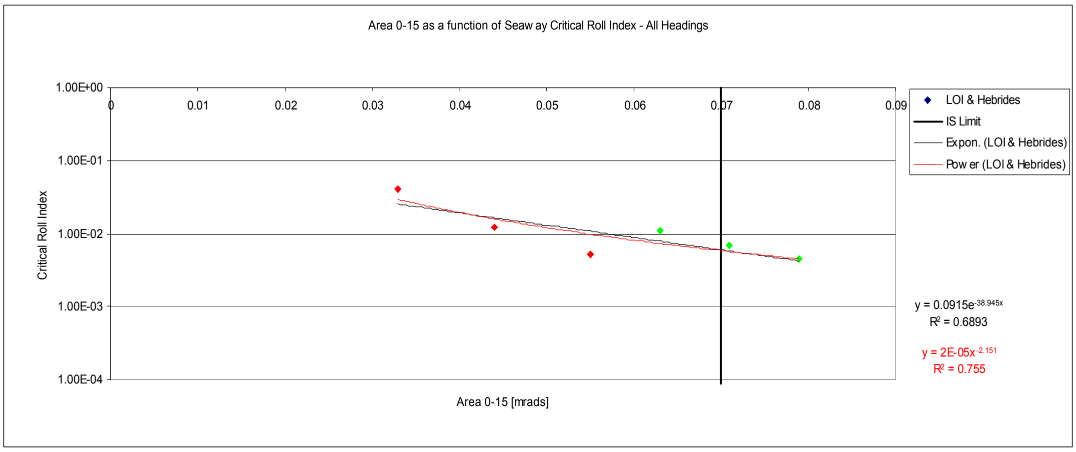

Figure D8 – Area 0-15 as a function of seaway Critical Roll Index

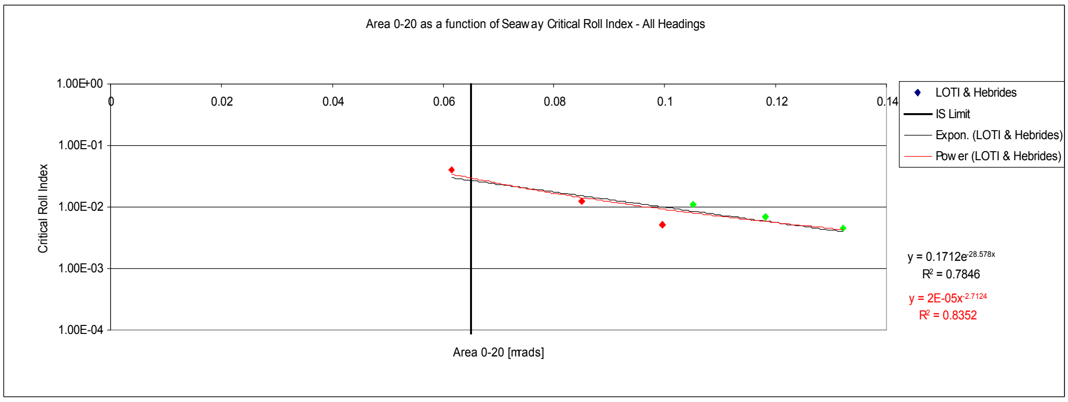

Figure D9 – Area 0-20 as a function of seaway Critical Roll Index

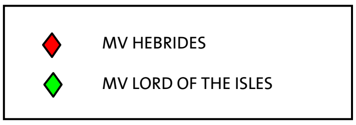

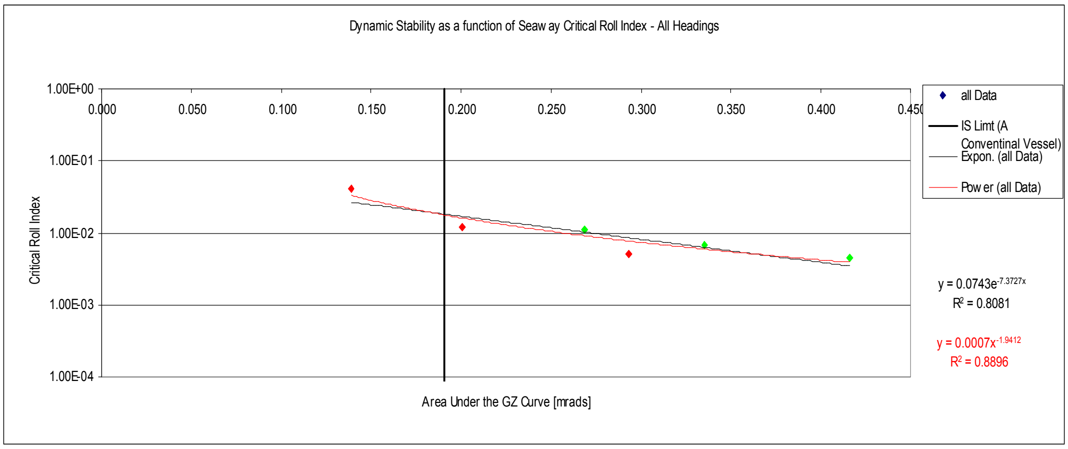

Figure D10 – Area under the GZ curve as a function of seaway Critical Roll Index

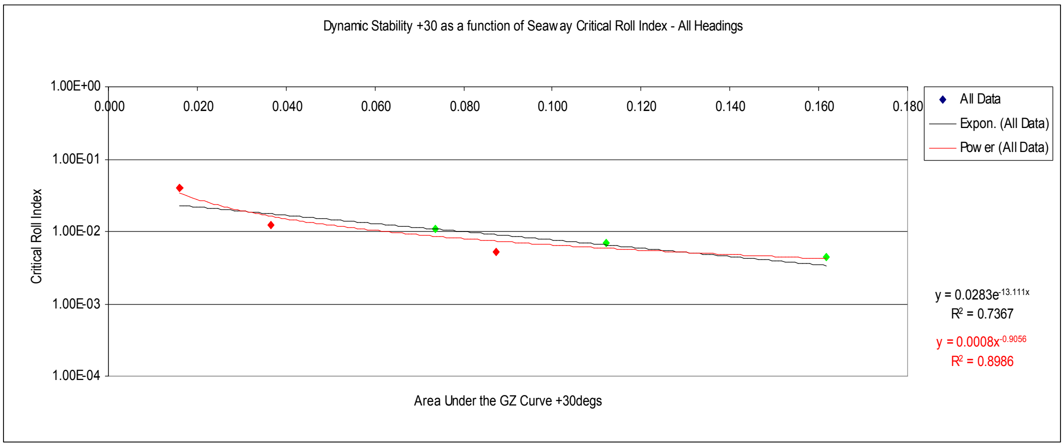

Figure D11 – Area under the GZ curve+30degs as a function of seaway Critical Roll

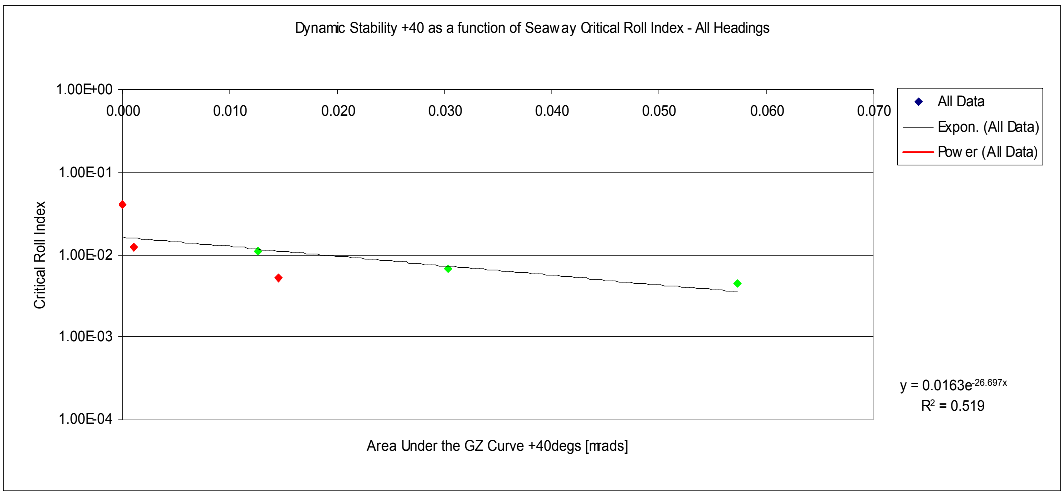

Figure D12 – Area under the GZ curve +40degs as a function of seaway Critical Roll

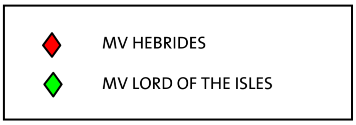

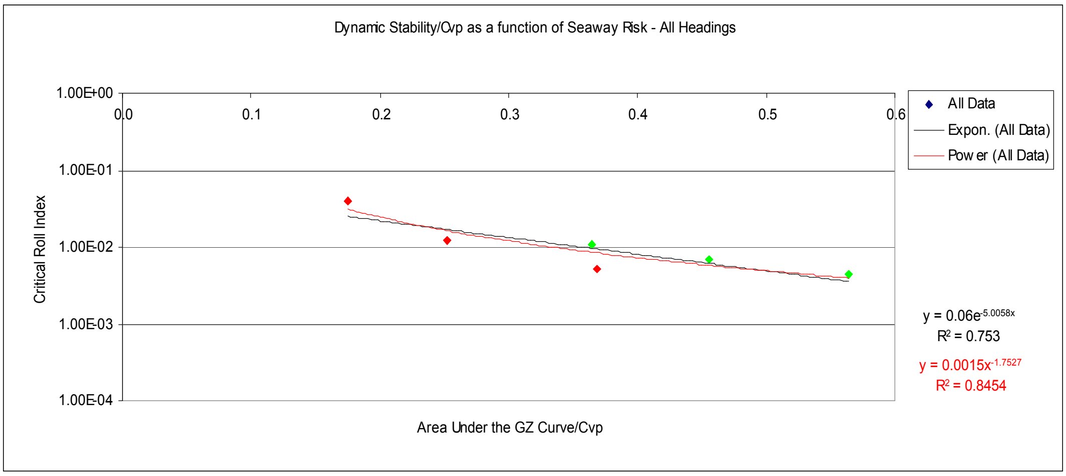

Figure D13 – Area under the GZ curve/Cvp as a function of seaway Critical Roll Index

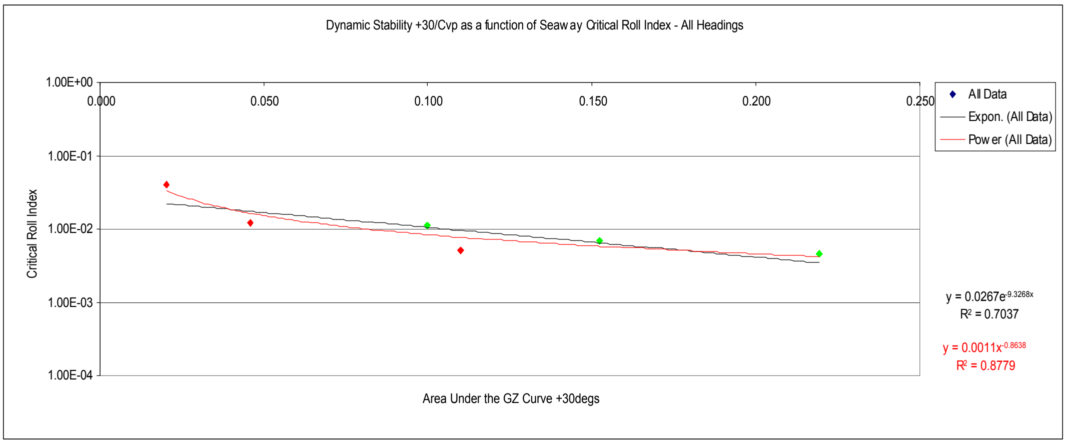

Figure D14 – Area under the GZ curve +30degs/Cvp as a function of seaway Critical

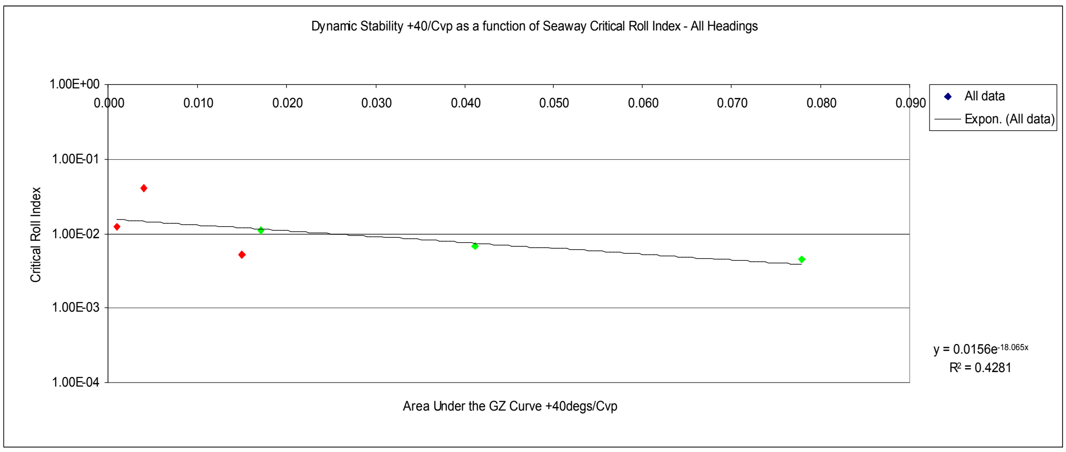

Figure D15 – Area under the GZ curve +40degs/Cvp as a function of seaway Critical

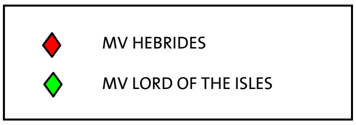

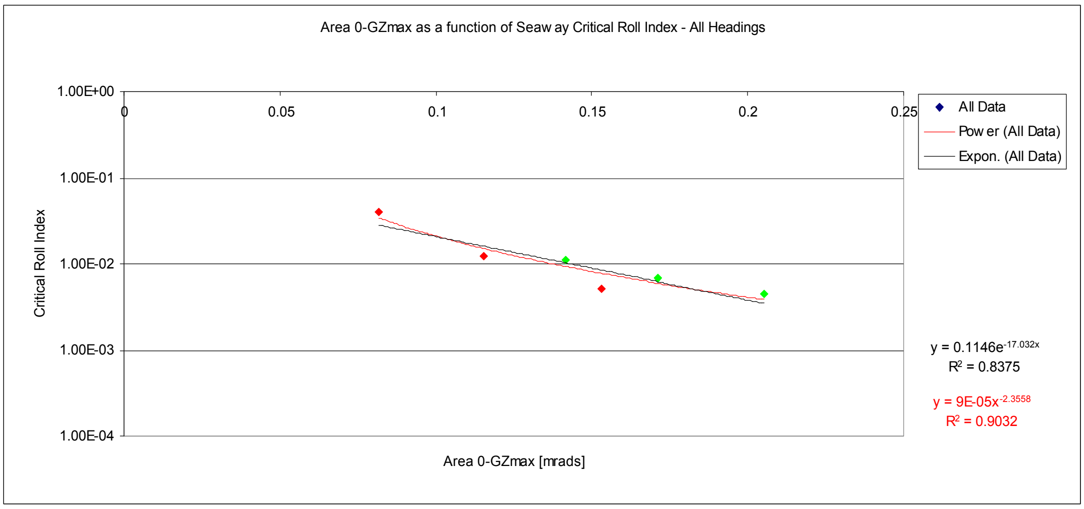

Figure D16 – Area under the GZ curve to GZmax as a function of seaway Critical Roll

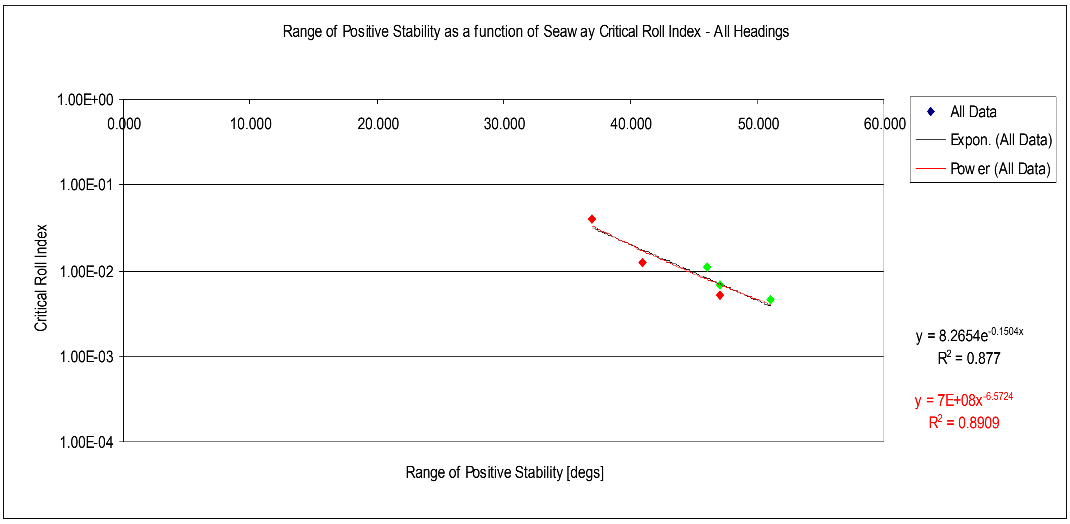

Figure D17 – Range of Positive Stability as a function of seaway Critical

Initial distribution list

External	
D. Foggie (MCA)	1
A. Scott (MCA)	2

QinetiQ	
A.Peters	3
J. Anderson (Project 572 File)	4
Information Resources	5

Blank page